Phospholipid Flippase Activity in Giant Plasma Membrane Vesicles and Rat Basophilic Leukemia-2H3 (RBL-2H3) Cells

A Thesis

Presented to the Faculty of the Graduate School

Of Cornell University

In Partial Fulfillment of the Requirements for the Degree of

Master of Science

By

Andrew Y. Chang

August 2014

ABSTRACT

Phospholipid flippase proteins regulate plasma membrane phospholipid asymmetry. Characterization of these transmembrane proteins is an ongoing area of research, as the mechanisms by which flippases function is poorly understood and the identification of proteins that exhibit flippase activity is incomplete.

We have investigated flippases activity in our giant plasma membrane vesicles (GPMVs) and intact RBL-2H3 cells. Results from our fluorescence quenching assays provide insight on flippase kinetics as well as flippase mediated phospholipid distribution across the membrane bilayer. With fluorescent annexin V binding assays, we also demonstrate that RBL-2H3 cells can be stimulated or perturbed in various ways that promote flippase mediated phosphatidylserine (PS) exposure on the cell surface. In particular, activated RBL-2H3 cells display distinctly punctate PS exposure, while cholesterol depleted cells exhibit sparse PS exposure on the membrane extracellular leaflet. Cells treated with the cysteine modification reagent N-ethylmaleimide (NEM) exhibit more uniform PS exposure at the cell surface, consistent with NEM-sensitive flippases. These studies further characterize the sensitivities of plasma membrane flippases and may potentially aid in the identification of additional proteins with flippase functionality.

BIOGRAPHICAL SKETCH

Andrew Y. Chang was born in the city of Paramount in Los Angeles County, California. Growing up in nearby Orange County, he attended Villa Park High School where he played on the basketball team and also competed in track and field. In 2005 he began attending the University of Southern California (USC) and earned his Bachelor of Science in Chemical Engineering in 2009. While at USC, he spent one year working in the Malmstadt Laboratory for Biomimetic Phase Interfaces studying the diffusion properties of supported lipid bilayers.

Andrew joined Anchen Pharmaceuticals in Irvine, California as a process engineer after completion of his undergraduate degree. Working in the Technical Services group, he contributed to multiple successful commercial product process validations. He left the company in 2012 to pursue his Master's degree in Applied Physics at Cornell.

DEDICATION

This thesis is dedicated to my mother for her overwhelming support and encouragement.

ACKNOWLEDGEMENTS

Foremost, I would like to thank my principle advisors Dr. David Holowka and Dr. Barbara Baird for the opportunity to conduct this research in their laboratory. Without their guidance and support, this work would not be possible. I am extremely grateful to have had the chance to learn from and work with such intelligent and kind people. I would also like to thank Dr. Manfred Lindau, my advisor in the department of Applied and Engineering Physics, for which his insightful comments and discussion have provided significant and unique perspectives on this research. Dr. Anant Menon and Dr. Michael Goren of the Weill Cornell Medical College also deserve considerable acknowledgment as their expertise has been invaluable to the progress of this project.

I also need to thank the current and former members of the Baird-Holowka laboratory: Roselynn Cordero, Marshall Colville, Marek Korzeniowski, Eshan Mitra, Jordan Mohr, Sarah Shelby, Alice Wagenknecht-Wiesner, Devin Wakefield, Marcus Wilkes, and Josh Wilson who have all contributed directly or indirectly to the development of this work. Lastly, I would like to thank my friends and family who have supported me during my time here at Cornell. Their encouragement has been essential to my survival here in Ithaca.

TABLE OF CONTENTS

LIST OF FIGURES

LIST OF TABLES

LIST OF ABBREVIATIONS

ABC	ATP-binding cassette
AF488	Alexa Fluor 488
AF555	Alexa Fluor 555
ATP	Adenosine triphosphate
BSA	Bovine serum albumin
DEPC	Diethylpyrocarbonate
DNP	Dinitrophenol
DTN	Dithionite
GPCR	G-Protein Coupled Receptor
GPMV	Giant Plasma Membrane Vesicle
IgE	Immunoglobulin E
MβCD	Methyl-β-cyclodextrin
NBD	Nitrobenzodiazole
NBD-PC	Nitrobenzodiazole phosphatidylcholine
NBD-PE	Nitrobenzodiazole phosphatidylethanolamine
NBD-PLs	Nitrobenzodiazole phospholipids
NEM	N-ethylmaleimide
OG	Octyl glucoside
PBS	Phosphate buffered saline
PC	Phosphatidylcholine
PE	Phosphatidylethanolamine
PS	Phosphatidylserine
RBL	Rat Basophilic Leukemia
SM	Sphingomyelin
TX-100	Triton X-100
ABC	ATP-binding cassette

CHAPTER 1 – INTRODUCTION

1.1 Cellular Membranes

Cellular membranes are semi-permeable physical barriers that separate the different cellular spaces. The plasma membrane envelopes the entirety of the cell to separate the extracellular environment from the intracellular environment. Intracellular organelles, in the case of eukaryotes, are surrounded by membranes that delineate the cytosolic space from the luminal space. By effectively compartmentalizing cells and cell structures, membranes allow for individualistic cell-by-cell or organelle-by-organelle regulation and function. Cellular membranes also serve as substrates for cellular activity including biochemical signaling and bulk transport via endocytosis or exocytosis.

1.2 Phospholipid Bilayer

Cell membranes are dynamic, fluid-like structures primarily composed of a phospholipid bilayer and membrane associated proteins (Figure 1). The majority of membrane lipids that comprise the bilayer are amphiphilic phospholipid (PL) molecules, each with a polar head group and non-polar hydrocarbon tail region (Figure 2). The phospholipids orient themselves into two distinct membrane leaflets that organize together with their hydrophobic tail groups associating with each other.

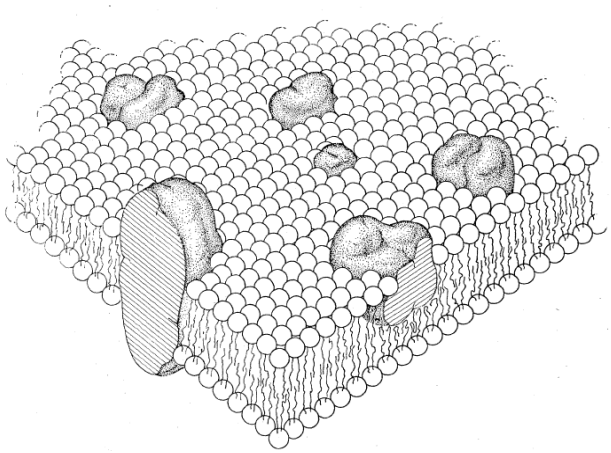

Figure 1 – Fluid mosaic model of the plasma membrane [1]

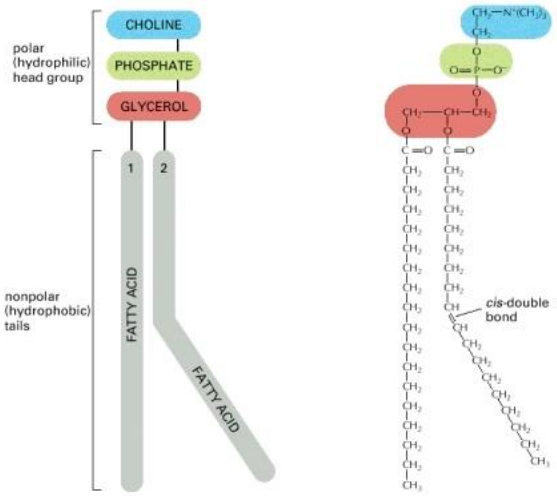

Figure 2 – Schematic and chemical composition of a phosphatidylcholine molecule [2]

The lipid composition of the plasma membrane of mammalian cells is primarily cholesterol and four major phospholipids: phosphatidylcholine (PC), sphingomyelin (SM), phosphatidylethanolamine (PE), and phosphatidylserine (PS) (Figure 3). The distribution of these phospholipid molecules across the bilayer membrane is asymmetric as the aminophospholipids PE and PS are found mostly sequestered to the inner (cytosolic) leaflet while PC and SM are located on the outer (extracellular) leaflet [3] (Figure 4). This phospholipid asymmetry has been found to be important for cellular recognition and signaling. For example, PS exposure to the outer leaflet has been found to be an indicator for apoptotic cells [4] and PS externalization in platelets is a known signal for blood coagulation [5]. In addition, control of phosphatidylinositol and its other phosphorylated forms at the plasma membrane is important for a variety of cellular functions and signaling [6]. The maintenance of phospholipid asymmetry is controlled by flippase membrane proteins that facilitate the transfer and organization of phospholipid molecules at the bilayer. Spontaneous phospholipid translocation across the bilayer is energetically unfavorable and does not occur at relevant physiological timescales [7].

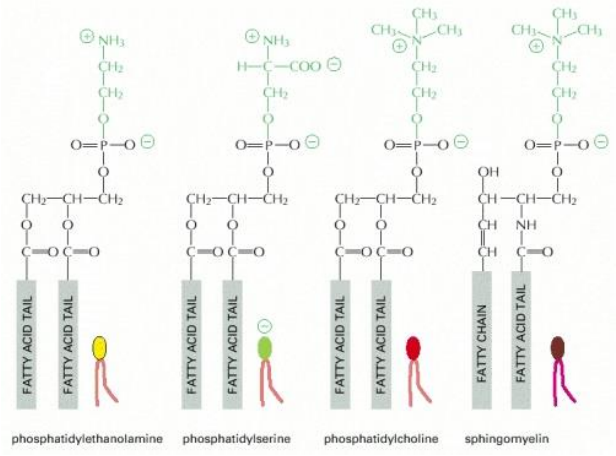

Figure 3 – Major PLs of the cell membrane [2]

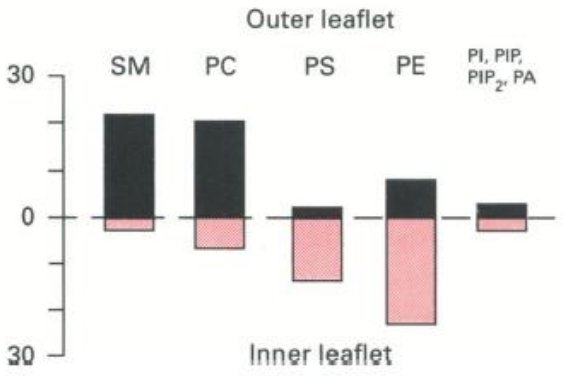

Figure 4 – PL distribution at the PM of a human erythrocyte membrane [3]

1.3 Flippases

Categorization of proteins that flip PL molecules across cellular membranes has typically been assigned by the direction of flipping as well as whether the mechanism is ATP-dependent or not. The three predominant categories of plasma membrane flippases are summarized in Table 1:

Primary Family	General Directionality	ATP-Dependent
P4-ATPase	Uni-directional (extracellular to cytosolic)	Yes
ABC Transporter	Uni-directional (cytosolic to extracellular)	Yes
Multiple	Bi-directional	No

Table 1 - Flippases in the plasma membrane

In the literature, it is common to find the term ‘flippase’ to represent membrane proteins that transfer phospholipids from the extracellular leaflet to the cytosolic leaflet while the term ‘floppase’ is often used to represent proteins translocating molecules in the reverse direction. In contrast, the term ‘scramblase’ is common for representing bi-directional, calcium activated phospholipid flipping proteins. In this document, the term ‘flippase’ will be used to describe any membrane protein that translocates phospholipids and specific categories of flippases will be

referenced by their particular directionality and ATP-dependence. The phospholipid distribution of the plasma membrane is thought to be maintained by uni-directional flippases while activated bi-directional flippases serve to breakdown the asymmetry of the bilayer [8].

1.3.1 Uni-Directional, ATP-dependent Flippases Maintain Plasma Membrane Asymmetry

Members of the P4-ATPase and ABC transporter families have been identified as uni-directional and ATP-dependent flippases. The different members of these particular families that exhibit flippase activity seem to differ in the phospholipids they are able to act upon.

The P-type ATPase superfamily of transmembrane proteins is involved with ion pumping and lipid translocation across cellular membranes via ATP hydrolysis (Figure 5) [9]. Members of the P4-ATPase subfamily, which in humans encode 14 genes [9], are known specifically as flippases that primarily engage in transferring phospholipids from the extracellular leaflet to the cytoplasmic leaflet in addition to functioning in vesicle transport pathways [10].

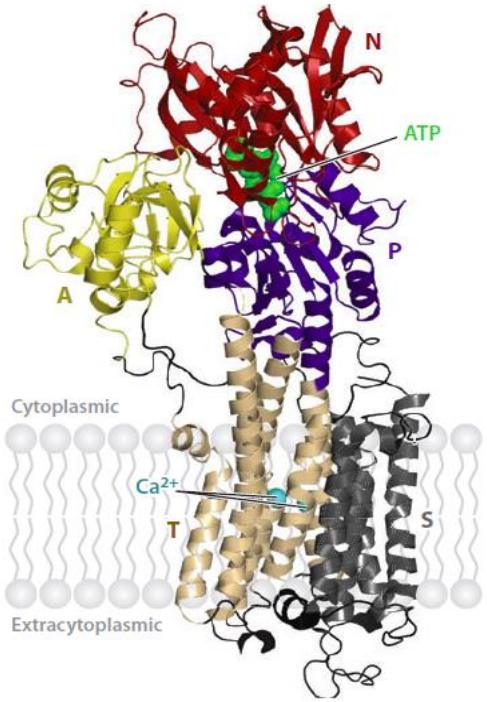

Figure 5 – Crystal structure of Ca^{2+} ATPase SERCA2a [9]

Zhou and Graham have demonstrated that purified and proteoliposome reconstituted Drs2p, a P4-ATPase from *Saccharomyces cerevisiae* primarily localized in the trans-golgi network, exhibits flippase activity specific to PS-analogues [11]. Yeast plasma membrane Dnf1p and Dnf2p have been shown to be necessary for inward flipping of PE, PS, and PC phospholipid

analogues using fluorescent lipid uptake assays [12]. Coleman and Molday were able to show that Atp8a2, a mammalian photoreceptor P4-ATPase, when reconstituted into lipid vesicles, was able to flip fluorescently labeled PS from the inner leaflet to the outer leaflet [13].

ATP-binding cassette (ABC) transporter proteins are involved with pumping various substrates across the membrane [14]. Some members of this family have been implicated in transferring phospholipids primarily from the cytosolic leaflet to the extracellular leaflet [15]. Members of the A, B and C subfamilies have been shown to flip a range of lipid molecules. ABCB1 (also known as multidrug resistant gene MDR1) has been demonstrated to translocate multiple short-chain lipid analogs, including PC and PE, while MDR3 (encoded by the ABCB4 gene) has been shown to specifically flip PC [16]. When reconstituted in liposomes, ABCA1 was found to flip PC, PS, and sphingomyelin while ABCA7 was found to preferentially flip PS [17]. ABCA4 has been shown to transport PE but from the extracellular leaflet to the cytoplasmic leaflet [17].

1.3.2 Bi-Directional, ATP-independent Flippases Disrupt Plasma Membrane Asymmetry

As energy dependent flippases serve to maintain certain phospholipid molecules on a particular side of the plasma membrane bilayer, inactivation of these uni-directional flippases and / or activation of bi-directional flippases are the primary means of rapid asymmetry breakdown. These bi-directional flippases, also referred to as 'scramblases' in the literature, are ATP-independent, Ca^{2+} activated proteins that are able to act on various lipid substrates [5, 18] (Figure 6).

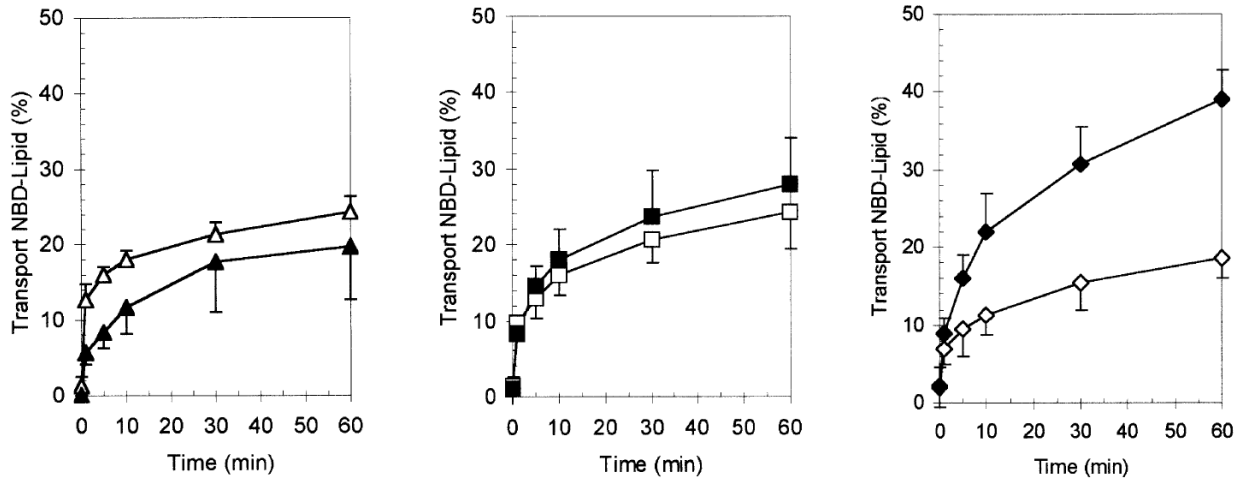

Figure 6 – Fluorescent NBD-PLs are observed to be bi-directionally transported across the membrane of red blood cells over a time course after Ca^{2+} / ionophore treatment [18]. Inward movement is displayed by filled data series and outward movement is shown as unfilled data series. Labeled phospholipids used were NBD-PS (triangles), NBD-PC (squares), and NBD-PE (diamonds).

The effort to identify plasma membrane proteins that exhibit bi-directional phospholipid movement has produced a few likely candidates. Phospholipid Scramblase 1 (PLSCR1) has been indicated as a likely Ca^{2+}-dependent flippase via fluorescence assays of reconstituted proteoliposomes [19, 20]. However, PLSCR1 knockout mice have demonstrated retention of scrambling activity [21] and other PLSCR1 deletion experiments suggest that PLSCR1 is not necessary for phospholipid scrambling [22]. Members of the transmembrane TMEM16 family have been demonstrated to function as phospholipid scramblers. Specifically, TMEM16F, 16C, 16D, 16G, and 16C were shown to flip a variety of phospholipids in Ca^{2+}-activated immortalized fetal thymocyte cell assays [23]. Purified afTMEM16F, of Aspergillus fumigatus, reconstituted in liposomes has been demonstrated to be both a Ca^{2+}-gated channel as well as a PL flippase [24]. The TMEM16 family proteins, also known as anoctamins, are ubiquitously expressed in mammalian cells and are commonly regarded as Ca^{2+}-activated ion channels [25] (Figure 7).

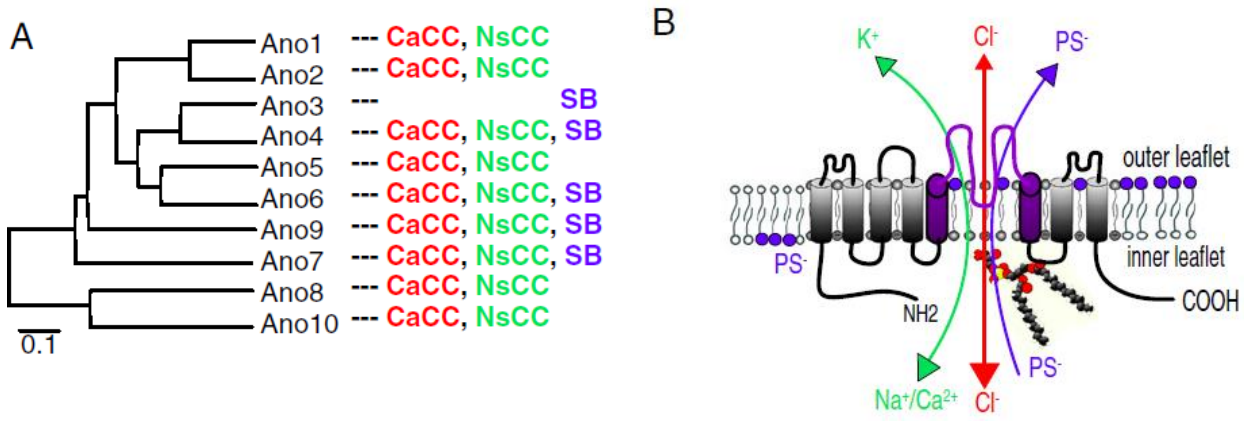

Figure 7 – (A) Anoctamins / TMEM16 members function as Ca^{2+}-activated Cl^--channels (CaCC), non-selective cation channels (NsCC), and phospholipid scramblases (PS). (B) Putative topology of Ano1 in the plasma membrane.[25]

Interestingly, the photoreceptor opsin of the G-Protein Coupled Receptor (GPCR) family has also been found to exhibit flippase activity in dithionite reduction assays in reconstituted proteoliposomes [26]. The existence of bi-directional flippases in both the TMEM16 and GPCR families suggest the possibility that other phospholipid scrambling proteins may exist in other distinct transmembrane protein groups.

1.4 Scope

A significant amount of plasma membrane flippase data has come from experiments using erythrocytes, platelets, and synthetic vesicles. In this study, we aimed to determine the level and nature of flippase activity in giant plasma membrane vesicles (GPMVs) derived from RBL-2H3 rat leukemic mast cell membranes and in intact RBL-2H3 cells. GPMVs, also known as blebs, are vesicles formed from the plasma membrane of mammalian cells [27, 28]. RBL-2H3 cells have been commonly used for the study of allergic responses [29] and, in particular, that stimulated with immunoglobulin E (IgE) initiates signaling through the high affinity IgE receptor

FcεRI [30]. Stimulated degranulation of RBL-2H3 cells has been demonstrated to expose PS on their surface, which can be monitored by annexin V binding [31].

The main objectives of this thesis research are to:

(i) Characterize flippase behavior in GPMVs and RBL-2H3 cells by measuring the kinetics of the flipping mechanism and also the flippase mediated phospholipid distribution of the plasma membrane.

(ii) Test ways to alter flippase activity by chemically modifying flippase proteins or via plasma membrane perturbations.

CHAPTER 2 – EXPERIMENTAL METHODS

2.1 Chemicals

Chain-labeled nitrobenzodiazole phospholipids (NBD-PLs) were purchased from Avanti Polar Lipids. Alexa Fluor 488 (AF488) Annexin V and Alexa Fluor 555 (AF555) Cholera Toxin B (CTB) were purchased from Molecular Probes. Sodium hydrosulfite (dithionite) was purchased from Sigma-Aldrich. RBL media consisted of minimum essential medium (MEM) with 20% fetal bovine serum (FBS) and 0.1% gentamicin. Tyrode's buffer (pH = 7.4) consisted of 135 mM NaCl, 5 mM KCl, 1 mM $MgCl_2$, 1.8 mM $CaCl_2$, 5.6 mM glucose, and 20 mM HEPES. GPMV buffer (pH = 7.4) consisted of 10 mM HEPES and 0.15 M NaCl.

2.2 Formation of GPMVs

GPMVs were chemically induced from RBL-2H3 cells by incubating the adherent cells with GPMV buffer, 2 mM $CaCl_2$, 2 mM dithiothreitol, and 25 mM formaldehyde for one hour at 37°C in a shaker bath at 60 RPM. The GPMVs form in suspension and are isolated by gently rapping the cell flask and depositing the supernatant into a separate container.

2.3 NBD-Quenching Assays

Quenching assays to measure flippase kinetics were performed using nitrobenzodiazole (NBD) conjugated phospholipid analogs. In these measurements, 900 μL of isolated GPMVs (Section 2.2) are first mixed with 100 μL of 10 mg/mL BSA in phosphate buffered saline (PBS) per sample. 12 – 20 μL of 0.2 mg/mL of NBD-PLs are added to each sample and quickly mixed. The

samples are then centrifuged at 18,000 RPM (38,724 g) for 30 minutes at 6°C then re-dispersed in GPMV buffer with NaN_3.

For quenching experiments using RBL-2H3 cells, the cells are first harvested by trypsinization and suspended in RBL media. The cells are then centrifuged at 900 RPM for 5 minutes and the pellet re-suspended in 6 mL of Tyrode's buffer with 1 mg/mL of bovine serum albumin (BSA). Samples are prepared by taking 1.5 – 2.0 mL of re-suspended cells and adding 10 – 20 μL of 0.2 mg/mL NBD-PLs in ethanol. The samples are allowed to equilibrate at room temperature for 1 minute then placed on ice for 10 – 15 minutes before an additional 2 mL of Tyrode's buffer is added and the samples are centrifuged again at 900 RPM for 5 minutes. Pelleted, NBD-PL labeled cells are then re-suspended in 2 mL of Tyrode's buffer. Samples for fluorimetry analysis are prepared by diluting 0.6 mL of the fluorescently labeled cells with 1.2 mL of Tyrode's buffer.

NBD-fluorescence quenching is measured at 10°C in a SLM 8100 fluorimeter in response to sample treatment with 20 mM freshly prepared dithionite anion ($S_2O_4^{2-}$) which irreversibly quenches the fluorescence (Figure 8) [32] or by titrations of cobalt divalent cations (Co^{2+}) which collisionally quench fluorescence [33, 34]. Excitation and emission wavelengths for NBD-fluorescence are $\lambda_{excitation}$ = 470 nm and $\lambda_{emission}$ = 530 respectively.

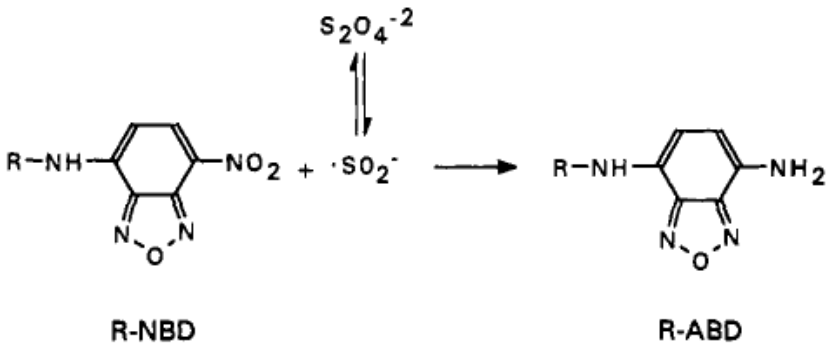

Figure 8 – Dithionite reduces the fluorescent 7-nitro-2,1,3-benzodiazole-4-yl-labeled phospholipids to non-fluorescent 7-amino-2,1,3-benzodiazol-4-yl-labeled phospholipids [32]

2.4 Cell Stimulation Assays

Cells were stimulated using a variety methods and flippase activity was assessed by monitoring surface exposed PS with fluorescent, Alexa Fluor-conjugated annexin V. Annexin V is a Ca^{2+}-dependent phospholipid binding protein with high affinity for PS [35].

2.4.1 Microscopy Assays

RBL cells were harvested by trypsinization and re-suspended in RBL media. The cells are then centrifuged at 900 RPM for 5 minutes and the pellet re-suspended in RBL media. For each sample, 0.5 mL of cells are plated in 35 mm MatTek coverslip dishes along with 1.5 mL of RBL media. Each sample was sensitized with 0.5 µg/mL of anti-DNP IgE overnight. The wells are washed with Tyrode's buffer then 1 mL of Tyrode's buffer was left in each microwell dish. Samples are treated for 20 minutes at room temperature with antigen (DNP-BSA, 0.8 µg/mL), 1µM A23187 calcium ionophore, 10 mM methyl-β-cyclodextrin, or 2.5 – 5.0 mM NEM along, in the presence of 20 µL of Alexa Fluor 488 – annexin V. After specified treatment, the samples are fixed using 4% para-formaldehyde + 0.1 % glutaraldehyde solution for 15-20 min, then stored in a 10 mg/mL BSA - PBS solution with 0.01% sodium azide. Select samples were stained with 2

μL Alexa Fluor 555 conjugated cholera toxin B, a GM1 binding protein. Samples were imaged at room temperature with a Zeiss LSM710 confocal microscope or a Leica DM-IRB inverted microscope using the appropriate filters.

CHAPTER 3 – RESULTS AND DISCUSSION

3.1 Kinetic Measurements and Determination of Flippase Activity in GPMVs

Flippase experiments in this study were initially conducted using GPMVs. These chemically induced membrane vesicles maintain the membrane proteins and lipid content that are originally in the plasma membrane from their derived cells [36] but are free from cytoskeletal constraints [37] that could potentially obscure flippase activity. To measure flippase activity, fluorescent NBD-PL analogs were exogenously incorporated into GPMVs and the extent of fluorescence quenching, used as a measure of phospholipid accessibility, was monitored with fluorescence quenching agents.

3.1.1 Dithionite Quenching Assays in GPMVs

GPMVs equipped with active flippase proteins are expected to take exogenously incorporated fluorescent phospholipids and distribute them in some manner across the inner and outer bilayer leaflets depending on the particular type of phospholipid analogue used. By adding membrane impermeable dithionite as an irreversible quenching agent, we would expect that fluorescent phospholipids situated in the extracellular leaflet to be quickly quenched. As the active flippases translocate the phospholipids across the bilayer, eventually all fluorescent NBD-phospholipids will at some point be exposed to the dithionite extracellular environment and near complete quenching should occur (Figure 9). GPMVs labeled with either NBD-phosphatidylethanolamine (NBD-PE) or NBD-phosphatidylcholine (NBD-PC) were observed to be nearly fully quenched over a time course upon addition of dithionite (Figure 10).

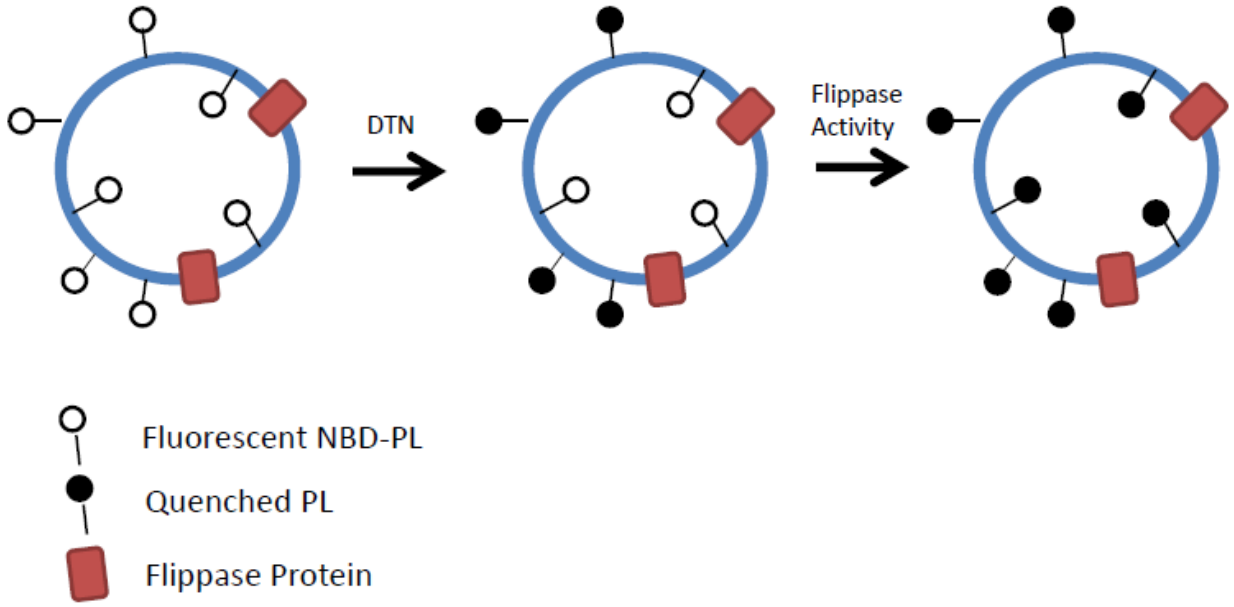

Figure 9 – In fluorescent NBD-PL labeled membranes, dithionite will irreversibly quench the exposed fluorescent phospholipids. Flippase membrane proteins will translocate phospholipids across the bilayer resulting in near complete quenching of the fluorescent probes.

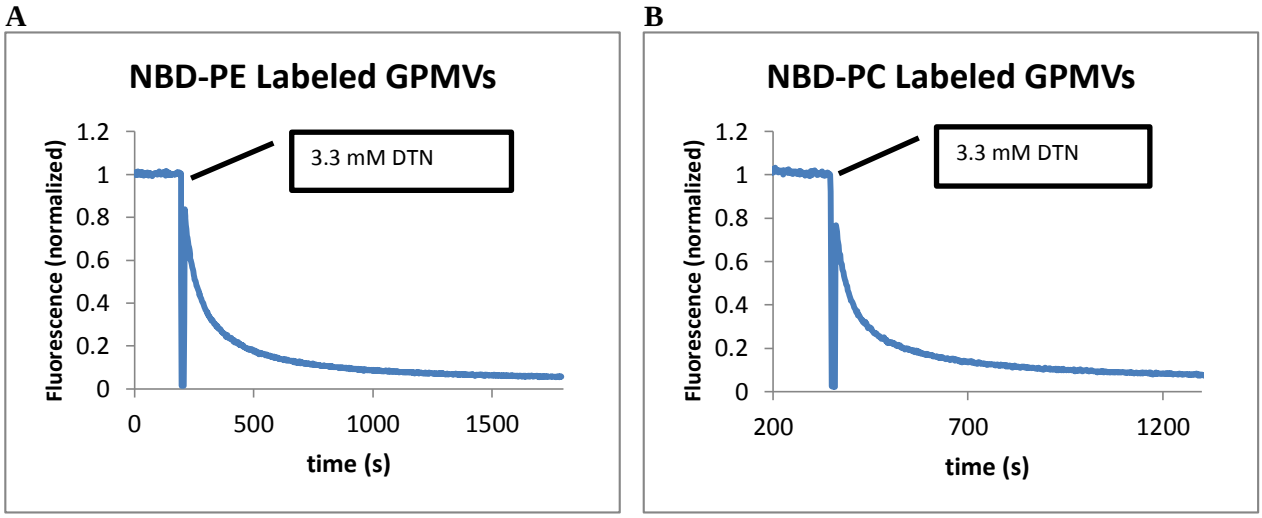

Figure 10 – Dithionite (DTN) quenching assay at 22°C of (A) NBD-PE and (B) NBD-PC fluorescently labeled GPMVs demonstrate near complete quenching.

Kinetics of the dithionite quenching behavior of the NBD-PE and NBD-PC labeled GPMVs can be evaluated by fitting the quenching trends to a single term exponential, a two term exponential, and a three component model (Figure 11). The proposed three component model is based on a

set of coupled differential equations that represent the fluorescent phospholipids at the inner leaflet, fluorescent phospholipids at the outer leaflet, and dithionite quenched fluorophores as follows:

$$PL_{in} \underset{k_{in}}{\overset{k_{out}}{\rightleftarrows}} PL_{out} \xrightarrow{k_{quench}} PL_{quenched}$$

PL_{in} = Fluorescent phospholipids at inner leaflet
PL_{out} = Fluorescent phospholipids at outer leaflet
$PL_{quenched}$ = phospholipids quenched by dithionite
k_i = representative rate constants

$$\frac{dPL_{in}}{dt} = k_{in}(PL_{out}) - k_{out}(PL_{in}) \qquad \text{Equation 1}$$

$$\frac{dPL_{out}}{dt} = k_{out}(PL_{in}) - k_{in}(PL_{out}) - k_{quench}(PL_{out}) \qquad \text{Equation 2}$$

$$\frac{dPL_{quenched}}{dt} = k_{quench}(PL_{out}) \qquad \text{Equation 3}$$

The coupled differential equations in this three component model are solved by numerical integration and the least-squares-fit to the data is performed by optimizing the representative rate constants k_{in}, k_{out}, and k_{quench} with the constraint that the constants must be greater than zero. The initial conditions of PL_{in} and PL_{out} are allowed to vary in the optimization with the constraint that initial PL_{in} + PL_{out} is equal to one, and initial $PL_{quenched}$ is set to zero as there is no quenching before addition of dithionite. We also see that if $k_{in} << k_{quench}$, then the fluorescence quenching can be represented by a two term exponential function (Equation 4) which may represent a physical interpretation of the two term exponential fit (Derived in Appendix A).

$$F(t) = a\exp(-k_{quench}t) + b\exp(-k_{out}t) \qquad \text{Equation 4}$$

Where $a = [PL_{out}]_i - \frac{k_{out}[PL_{in}]_i}{k_{quench}-k_{out}}$ and b = (1 – a) = $[PL_{in}]_i + \frac{k_{out}[PL_{in}]_i}{k_{quench}-k_{out}}$

A

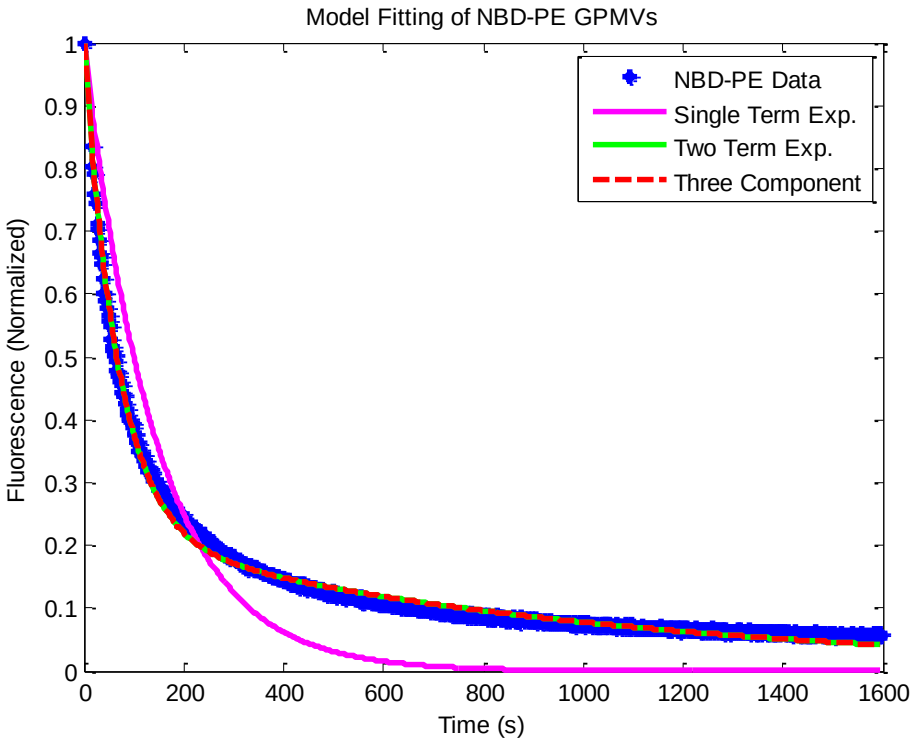

B

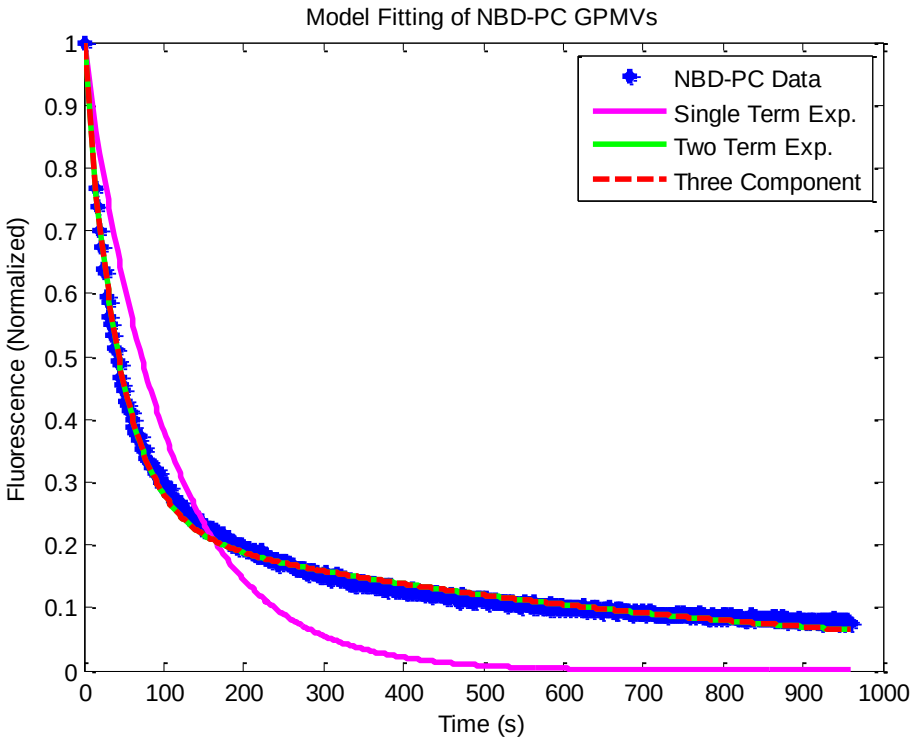

Figure 11 - Single term exponential, two term exponential, and three component model fits for (A) NBD-PE labeled GPMVs and (B) NBD-PC labeled GPMVs

We find that the dithionite quenching results for both NBD-PE and NBD-PC labeled GPMVs fit well to the two term exponential function and the three-component model as opposed to the single term exponential function (Table 2). This may indicate that the total quenching behavior is attributed to multiple components that could represent dithionite reduction of NBD fluorescence and flippase activity. In both the two term exponential function and the three component model, we find that the rate of quenching due to dithionite reduction is rather rapid ($t_{1/2,\ quench} < 1$ minute) compared to the rate of outward flipping ($t_{1/2,\ out}$ = approximately 8 - 11 minutes) where the half-times are calculated by $t_{1/2} = \ln(2)/k_i$ with k_i being the respective rate constant. These fits also indicate that the inward rate of flipping is rather slow, however the accuracy of these values is questionable possibly due to the rapid nature of dithionite reduction. For example, in the case that the rate of dithionite reduction is near instantaneous, we would only be able to measure fluorescence decay due to outward flipping. Although inward flipping still may occur, this rate would be obscured as only quenched fluorophores would be flipped inwards which cannot be directly measured in our assay.

We also find that the best fit initial distribution of phospholipids before addition of dithionite is approximately 20% at the inner leaflet and approximately 80% at the outer leaflet for both NBD-PE and NBD-PC labeled GPMVs.

Single Term Exponential $F(t) = e^{kt}$

Label	k (s^{-1})	$t_{1/2}$ (s)	R^2
NBD-PE	0.006935	99.95	0.6108
NBD-PC	0.009653	71.81	0.3387

Two Term Exponential $F(t) = ae^{-k_{quench}t} + be^{-k_{out}t}$

Label	a	b = 1 - a	$(PL_{in})_i$	$(PL_{out})_i$	k_{quench} (s^{-1})	k_{out} (s^{-1})	$t_{1/2,kquench}$ (s)	$t_{1/2,kout}$ (s)	R^2
NBD-PE	0.7771	0.2229	0.2071	0.7929	0.01484	0.001052	46.71	658.9	0.9926
NBD-PC	0.7625	0.2375	0.2237	0.7763	0.02345	0.00136	29.56	509.7	0.9938

Three-Component Model

Label	$(PL_{in})_i$	$(PL_{out})_i$	k_{quench} (s^{-1})	k_{in} (s^{-1})	k_{out} (s^{-1})	$t_{1/2,\ kquench}$ (s)	$t_{1/2,\ kin}$ (s)	$t_{1/2,\ kout}$ (s)	R^2
NBD-PE	0.1997	0.8003	0.0147	0.0001	0.0011	47.15	6,931	630.1	0.9929
NBD-PC	0.2158	0.7842	0.0232	0.0002	0.0014	29.88	3,466	495.1	0.9939

Table 2 – Single term exponential, two term exponential, and three-component model fit parameters for NBD-PE and NBD-PC labeled GPMVs. Half-times ($t_{1/2}$) = ln(2)/ki, where k_i represents the respective rate constants k, k_{in}, k_{out}, and k_{quench}.

The data analysis for these dithionite quenching assays must be interpreted with the following considerations: firstly that dithionite may not be completely membrane impermeable and secondly, that the GPMVs may not have distributed the exogenously incorporated NBD-PLs at some equilibrium distribution before addition of the quenching agent.

If dithionite is permeable to some extent and able to directly access fluorescent phospholipids at the inner membrane leaflet, the mechanism of the proposed models would not be absolutely accurate and the fitted rate constants and initial phospholipid distributions would not be completely reliable. This does not dismiss observable flippase activity as it still suggests some inner and outer leaflet distribution of fluorescent phospholipids, although it may be possible that

some slower quenching component seen in our models is attributed to dithionite leaking across the membrane. Separate assays for measuring dithionite permeability would be necessary in order to address this concern. Additionally, if the vesicles have not reached a steady state distribution of NBD-PLs before beginning the assay, the best fit initial inner leaflet and outer leaflet fluorophore populations would not represent the equilibrium phospholipid distribution. A potential experiment to assess the necessary time for a steady state phospholipid distribution may be to conduct dithionite assays at a variety of incubation times after addition of the NBD-PLs. These types of experiments may also provide a clearer indication of the inward flipping rate constant.

These particular considerations must be addressed in order to make definitive quantitative conclusions on the best fit rate constants and initial phospholipid distributions however, we may still be able to qualitatively conclude that the near complete quenching behavior observed in the NBD-PE and NBD-PC labeled GPMVs suggests multiple components in the quenching kinetics and one of these components may be attributed to flippase activity.

3.1.2 Collisional Quenching Assays in GPMVs

Collisional quenching assays may be used to assess how phospholipids are being distributed about the membrane. Here, GPMVs were labeled with fluorescent NBD-PE and titration experiments using cobalt (II) chloride [38], a collisional quencher that quenches fluorescence when in contact with fluorophores, were performed (Figure 12). In these experiments, we would expect some fraction of NBD-PE to be sequestered at the inner leaflet, as it is in plasma membranes, and thus inaccessible to the collisional quencher. Demonstration of this effect along

with our dithionite quenching experiments would further indicate that we may be observing flippase activity in our GPMVs.

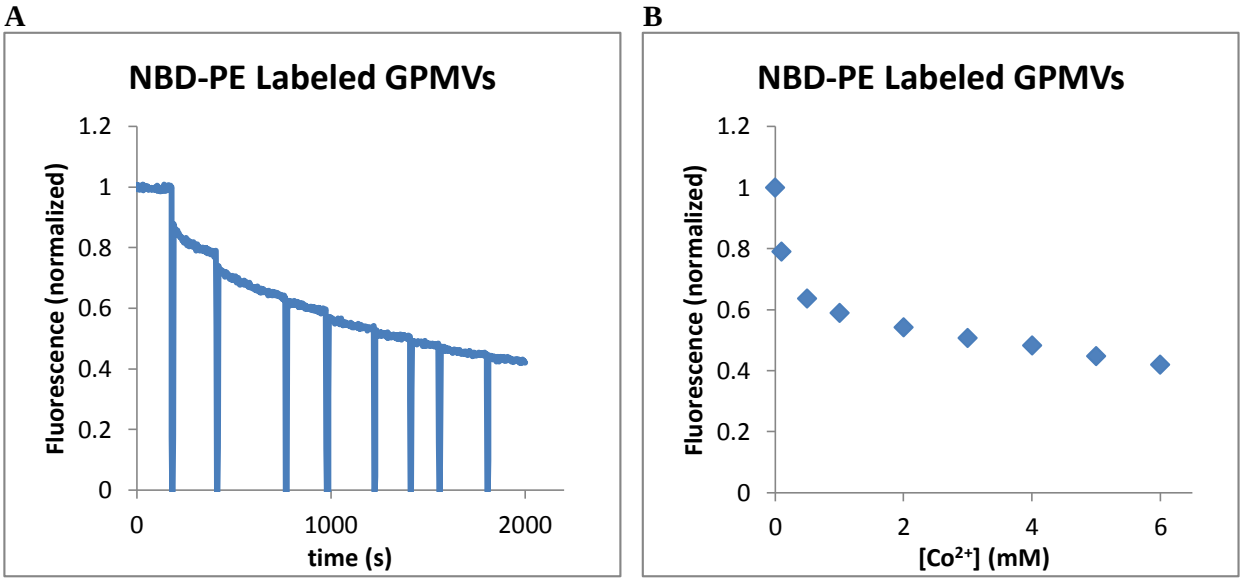

Figure 12 – GPMVs labeled with NBD-PE and (A) titrated at 22°C with sequential additions of Co^{2+} at 0.1 mM, 0.5 mM, 1 mM, 2 mM, 3 mM, 4 mM, 5 mM, and 6 mM total concentrations. (B) The fluorescence titration data is plotted as a function of Co^{2+} concentration and seen to display a bi-phasic quenching behavior.

Using the Co^{2+} collisional quencher, the quenching of the fluorescently labeled GPMVs seems to converge to some non-zero fluorescence signal in our titrations (Figure 12B), suggesting that we are observing flippase mediated distribution of phospholipids in our GPMVs . However, it is of some concern that we do not reach a complete 'steady-state' level and rather observe a slow, linear quenching behavior at higher concentrations of Co^{2+} which possibly indicates that the cations are slightly permeable to the GPMVs. In addition, the fluorescence signal does not completely stabilize upon each addition of Co^{2+} (Figure 12A) which further raises concerns regarding membrane permeability of the collisional quencher. This permeability of the Co^{2+} could potentially be due to cation channels or defects in the membrane.

Instead of titrations of Co^{2+} into one sample of GPMVs, individual samples of fluorescently labeled GPMVs were identically prepared and the quenching behavior was examined upon single treatments of different concentrations of Co^{2+} (Figure 13A). As expected, we observe more quenching at higher concentrations of quencher, but we also see that the quenching does not quickly stabilize upon addition of the quencher and a steady state is never completely reached. We can choose a time point near the beginning (approximately 30 seconds after addition of the quencher) and near the end of our experiment (approximately 1,200 seconds after addition of the quencher) and compare the fluorescence quenching at equal time points as a function of quencher concentration (Figure 13B). Once again, we observe a rather bi-phasic behavior where there is a fast quenching response at lower quencher concentrations and a slower continuous response at higher quencher concentrations. This may further indicate that the GPMVs are slightly permeable to the collisional quencher, most notably at the higher Co^{2+} concentrations.

A

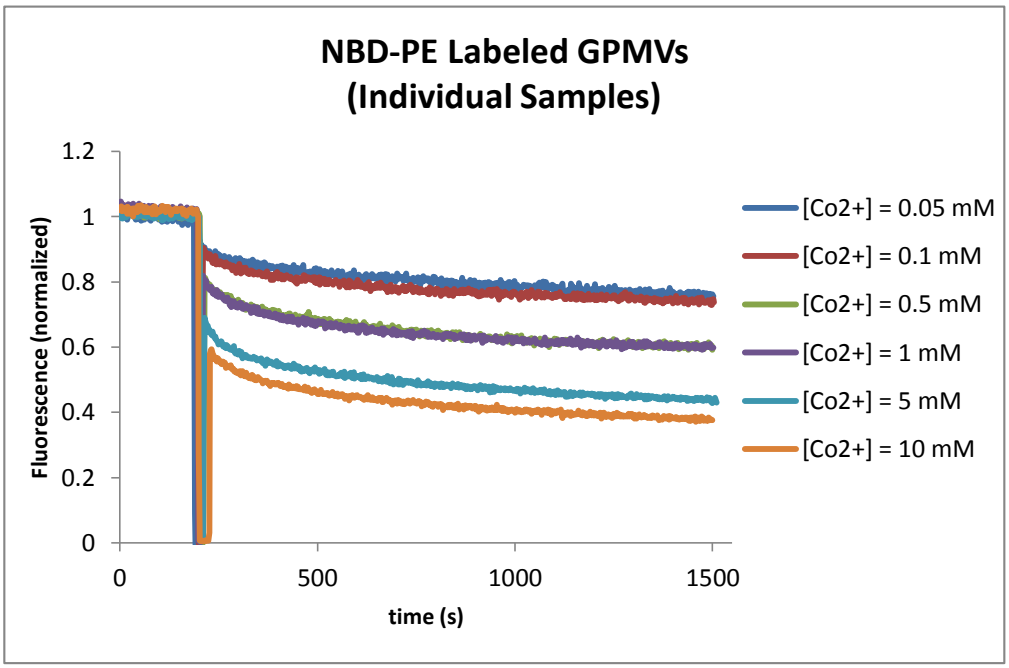

B

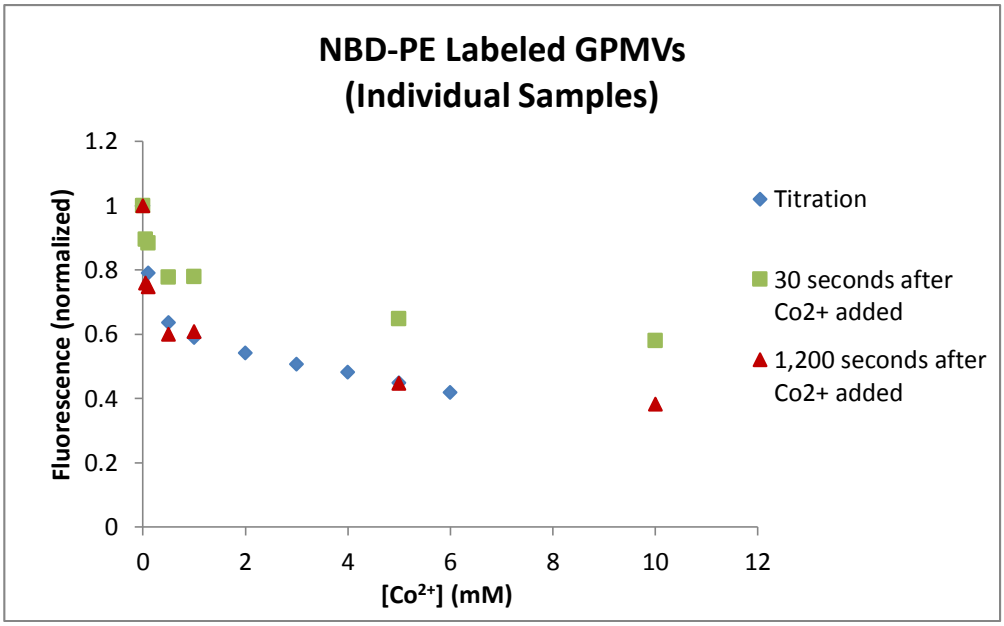

Figure 13 – (A) The quenching behavior of fluorescently labeled GPMVs is observed in separate samples treated with different concentrations of Co^{2+} collisional quencher. (B) The fluorescence data from the individually tested samples at approximately 30 seconds and 1,200 seconds after addition of the quencher is plotted as a function of Co^{2+} which exhibits a bi-phasic quenching behavior with a fast quenching response at lower concentrations and a slow response at higher concentrations. For comparison, the titration data from Fig. 12B is also plotted.

These collisional quenching experiments can also be analyzed using the Stern-Volmer relationship (Equation 5) where fluorescence quenching is expressed as a function of quencher concentration (Figure 14). A 'plateau' behavior in the Stern-Volmer plots is indicative of having a population of fluorophores being inaccessible to the collisional quencher while linear behavior indicates that nearly all of the fluorophores are accessible.

$$\frac{F_0}{F} = 1 + k_{sv}[Q] \qquad \text{(Equation 5)}$$

where F_o = initial fluorescence (absence of quencher), F = fluorescence, k_{sv} = Stern-Volmer constant and [Q] = Quencher concentration

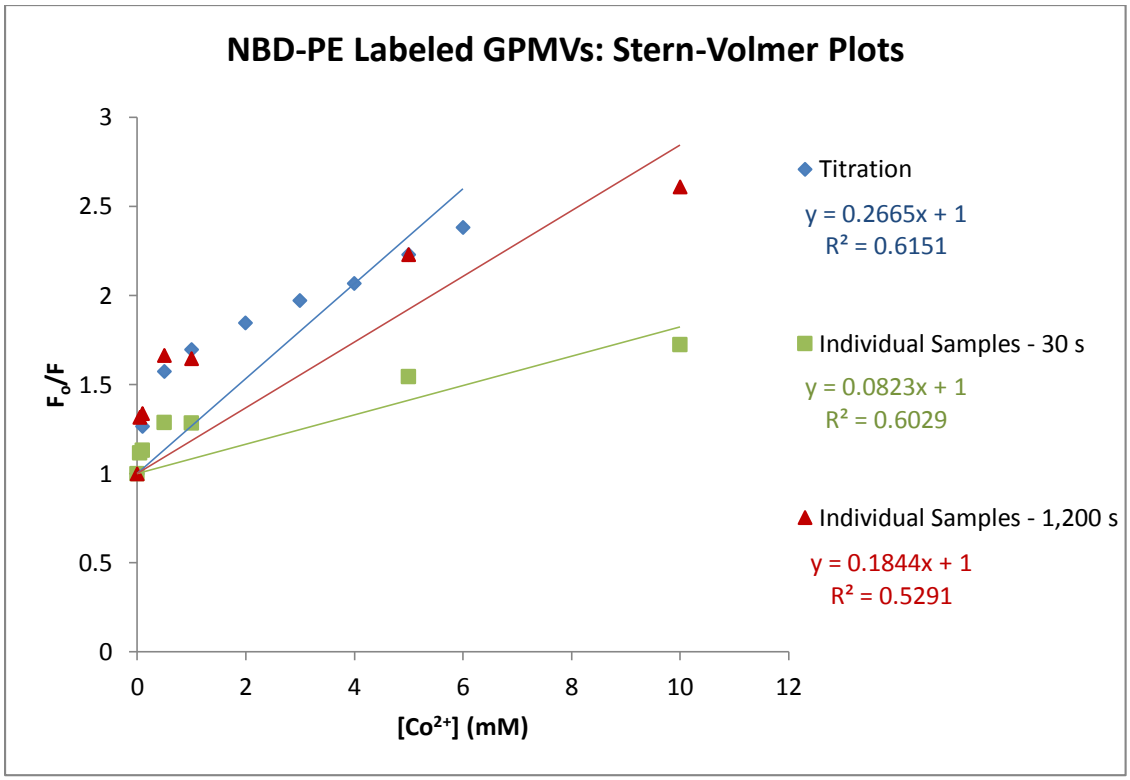

Figure 14 – Fluorescence data from the Co^{2+} titration assay (Figure 12) and individual sample quenching data (Figure 13) is plotted as a function of quencher concentration via the Stern-Volmer relationship. The non-linear nature of the data indicates that some fraction of NBD-PE fluorescent phospholipids is less accessible to the collisional quencher, possibly because a fraction of the NBD-PE fluorophore is flipped to the inner bilayer leaflet. However, the fact that the fluorescent quenching does not completely level off at higher quencher concentrations may indicate that the cations are slightly permeable to the GPMVs.

The Stern-Volmer relations can also be modified (Equation 6) to calculate a fraction of accessible fluorophores (f_a) representing the NBD-PE that may be exposed on the outer leaflet (Figure 15, derivation in Appendix B). The y-axis intercept of these plots represents the inverse fraction of accessible fluorophores, which in the absence of quencher membrane permeability, may correlate with fluorophores being maintained at the extracellular bilayer leaflet.

$$\frac{F_o}{\Delta F} = \frac{1}{f_a}\frac{1}{K_{sv}[Q]} + \frac{1}{f_a} \qquad \text{(Equation 6)}$$

where F_o = initial fluorescence, $\Delta F = F_o$ – measured fluorescence, k_{sv} = Stern-Volmer constant, f_a = fraction of quencher accessible fluorophores, and [Q] = Quencher concentration

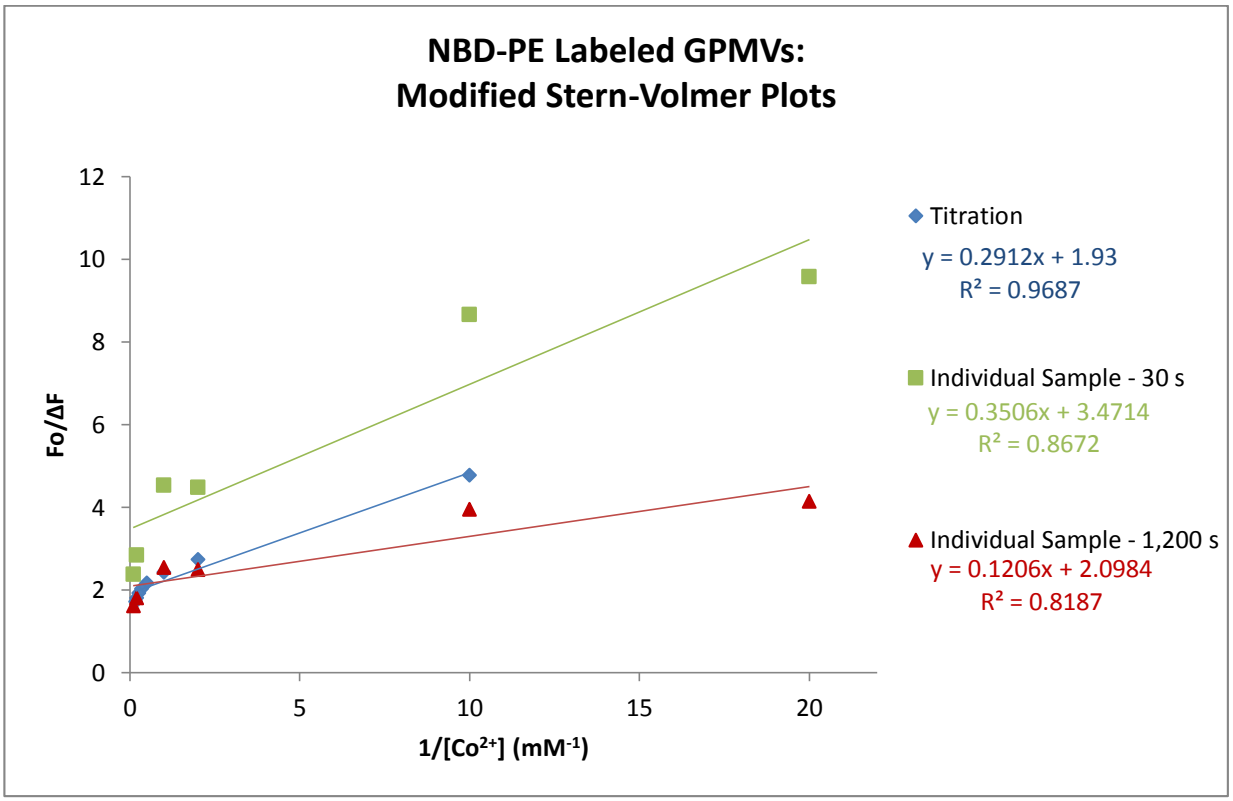

Figure 15 – The Stern-Volmer relation is modified in order to provide a linear function for calculating the fraction of accessible fluorophores that should correspond to fluorophores maintained on the outer leaflet. Here we find that the fraction of quencher accessible fluorophores (f_a) is approximately 52%, 29%, and 48% for the Co^{2+} titrated sample, individually treated samples at 30 seconds after quencher addition, and individually treated samples at 1,200 seconds after quencher addition, respectively.

Using the modified Stern-Volmer relations, we are able to calculate that approximately 30 - 50% of the NBD-PE in our GPMVs seems to be accessible to the Co^{2+} quencher. We also see that in our modified Stern-Volmer relations, the linear fit is heavily weighted to low concentration values due to the dependency of the inverse concentration of Co^{2+} which may introduce some bias in the calculated fraction of quencher accessible fluorophores. Another consideration that must be accounted for is the possibility that the fluorescently labeled GPMVs have not been given enough time to distribute the exogenously added NBD-PE to some equilibrium state which may allow for more fluorescent phospholipids to be accessible at the early time points of our experiment. These concerns regarding potential quencher membrane permeability, biased data weighting in our modified Stern-Volmer analysis, and steady state considerations limit our interpretation of these results as only a qualitative indication that active flippases may be distributing the fluorescent NBD-PE across the bilayer in some manner.

Another possible method to determine whether flippases are actively translocating the fluorescent NBD-PLs across the GPMV bilayer is to permeabilize the vesicles after incorporation of the fluorescent phospholipid analogs. Membrane permeabilization would allow direct access of the collisional quencher to the fluorescent phospholipids situated in the inner leaflet and we would expect to see enhanced quenching. Saponin is a detergent that can interact with cholesterol and create small holes in membranes [39]. By treating NBD-PE labeled GPMVs with varying concentrations of saponin, then conducting a collisional quenching titration with Co^{2+}, we observe a slightly enhanced quenching effect (Figure 16). However, we would expect that if the GPMVs were effectively permeabilized, we should observe a more significant enhanced quenching effect than what is detected.

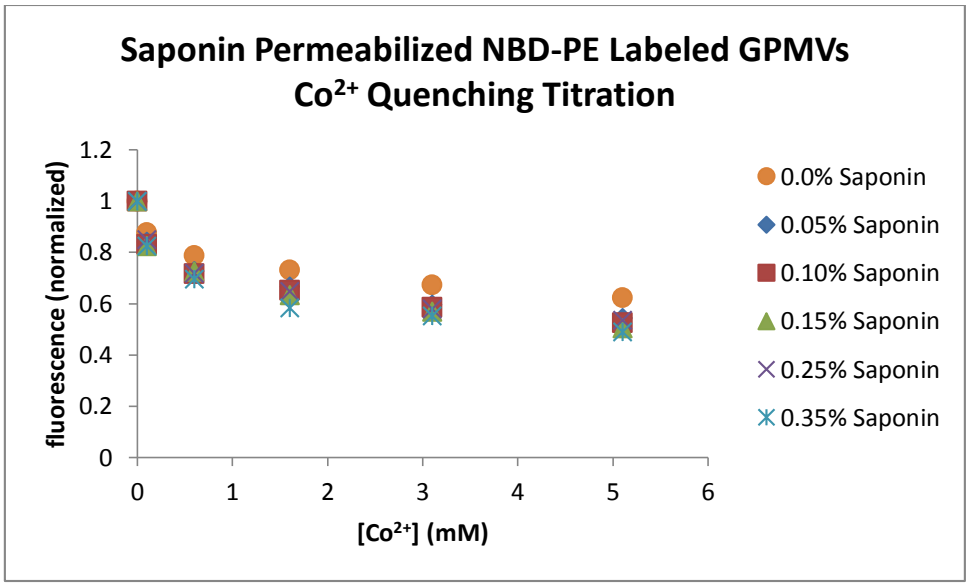

Figure 16 – GPMVs are labeled with NBD-PE then permeabilized with saponin at varying concentrations. A collisional quenching assay is then performed using Co^{2+}. Higher concentrations of saponin show a slightly enhanced quenching effect.

GPMVs can also be permeabilized using Triton X-100 (TX-100) or octyl glucoside (OG) detergents. However, it was found that when GPMVs with incorporated NBD-PLs were treated with these detergents, the fluorescence signal was dramatically enhanced to saturated levels (Figure 17). This may be due to the fluorescent phospholipids being solubilized into a micelle environment which has less intrinsic fluorescence quenching effects than the GPMV bilayer environment. In addition, the quenching behavior of the OG detergent solubilized GPMVs was found to be much less sensitive to the quenching effects of Co^{2+} (Figure 18), which further diminished the usefulness of this technique in determining flippase-mediated phospholipid distribution.

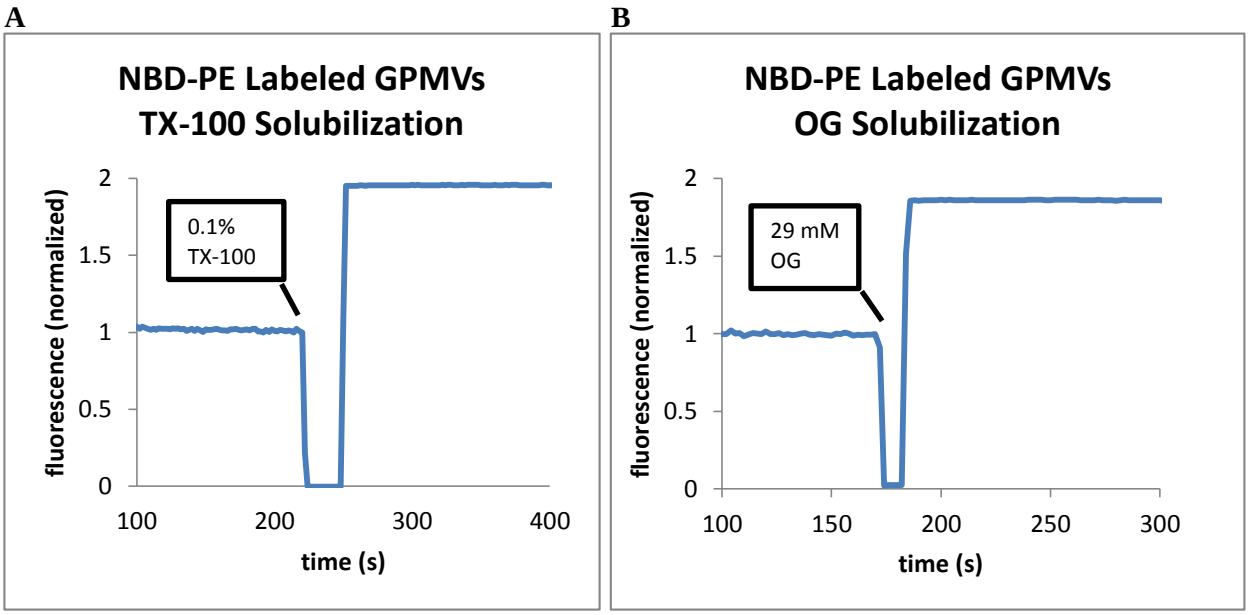

Figure 17 – (A) TX-100 and (B) OG Permeabilization GPMVs demonstrate a sudden increase of fluorescence to saturated fluorescence levels.

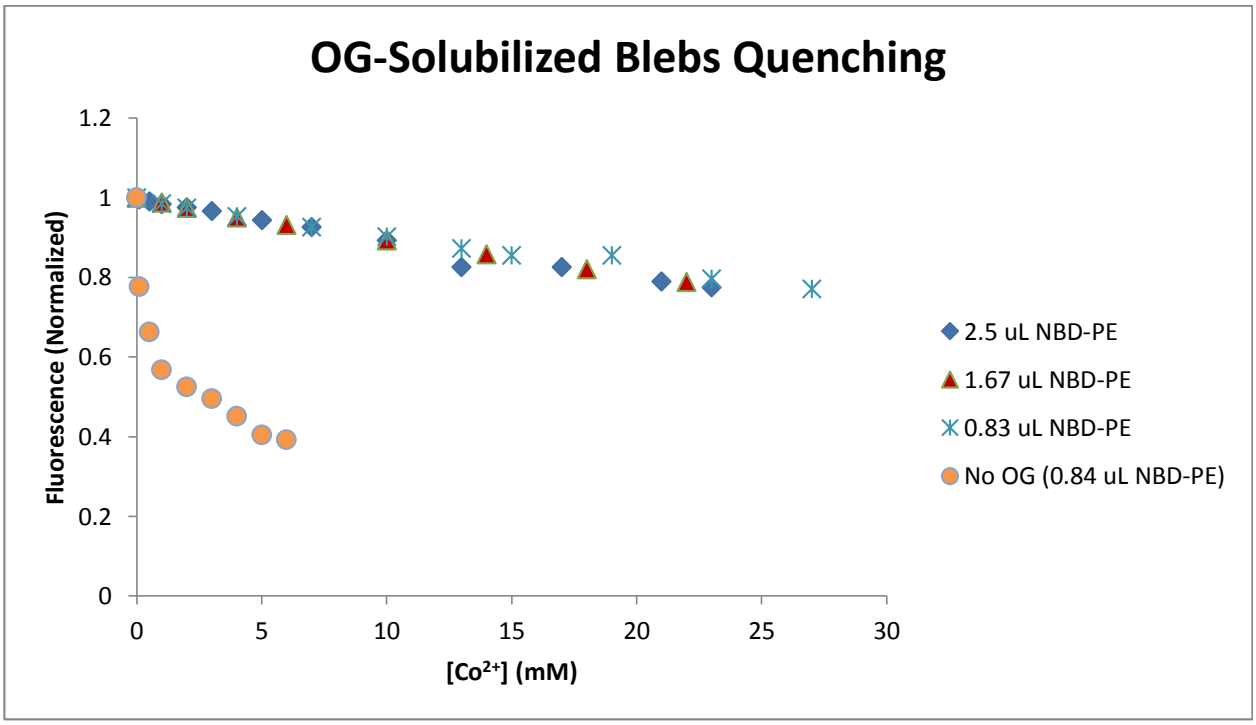

Figure 18 – Co^{2+} quenching behavior of OG detergent solubilized and non-solubilized NBD-PE labeled GPMVs at various fluorophore amounts demonstrate the insensitivity of the solubilized GPMVs to the Co^{2+} quencher as compared to the non-solubilized GPMVs.

3.2 Kinetic Measurements and Determination of Flippase Activity in RBL-2H3 Cells

Flippase activity was examined using RBL-2H3 cells by the same quenching assays as those in the GPMV models. Quenching experiments were conducted at 10°C to prevent endocytosis. As with the GPMVs, upon exogenous incorporation of NBD-PLs, active flippases would operate to distribute the fluorescent phospholipid analogs in some particular manner across the membrane bilayer leaflets. Dithionite quenching assays were conducted in which flippase activity is expected to facilitate near complete quenching of the fluorescently labeled cells as depicted in Figure 9. Collisional quenching assays using Co^{2+} are expected to only quench fluorophores that are maintained at the membrane extracellular leaflet and therefore provide an indication of the flippase mediated distribution of phospholipid molecules across the membrane bilayer. Together, the dithionite and collisional quenching assays offer kinetic and functional information of the flippase activity in RBL-2H3 cells.

3.2.1 Dithionite Quenching Assays in RBL-2H3 Cells

Dithionite quenching of both NBD-PE and NBD-PC fluorescently labeled RBL-2H3 cells demonstrate near complete quenching (Figure 19). The dithionite quenching behavior was evaluated by fitting the quenching trends to a single term exponential, a two term exponential, and a three component model as described in Section 3.1.1 (Figure 20).

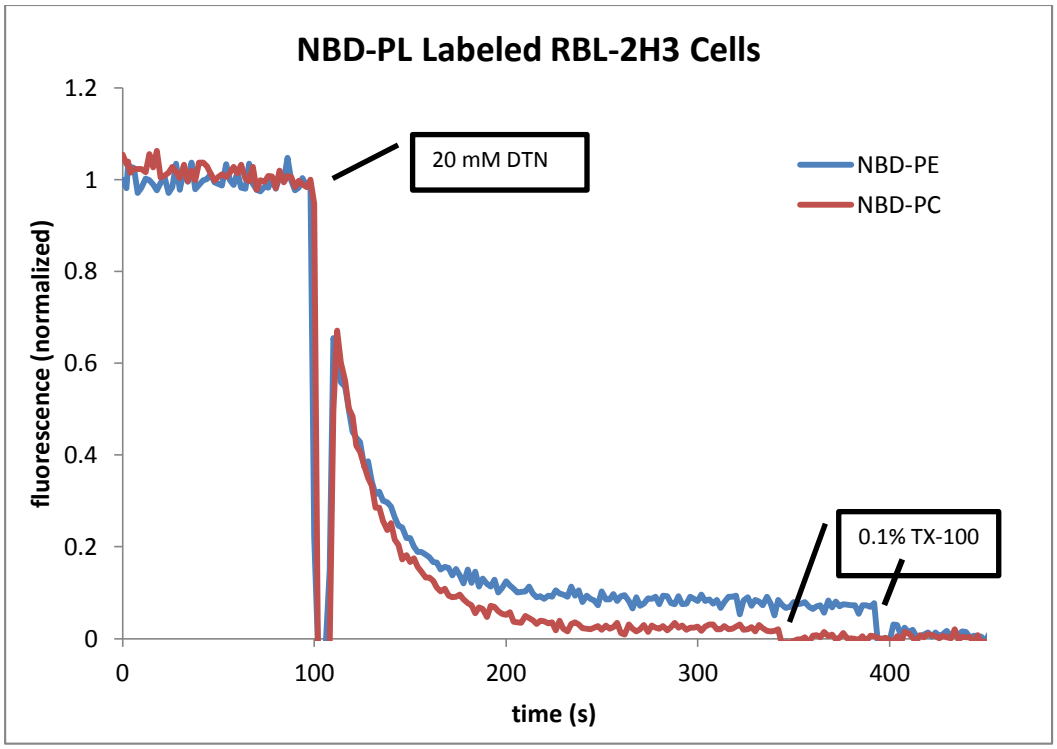

Figure 19 – Dithionite quenching assay at 10°C with NBD-PE and NBD-PC labeled RBL-2H3 cells show that near complete quenching is achieved over time. Triton X-100 was added when the fluorescence signal leveled out. Detergent permeabilization of the cells seemed to allow for quenching of the remaining fluorescence.

A

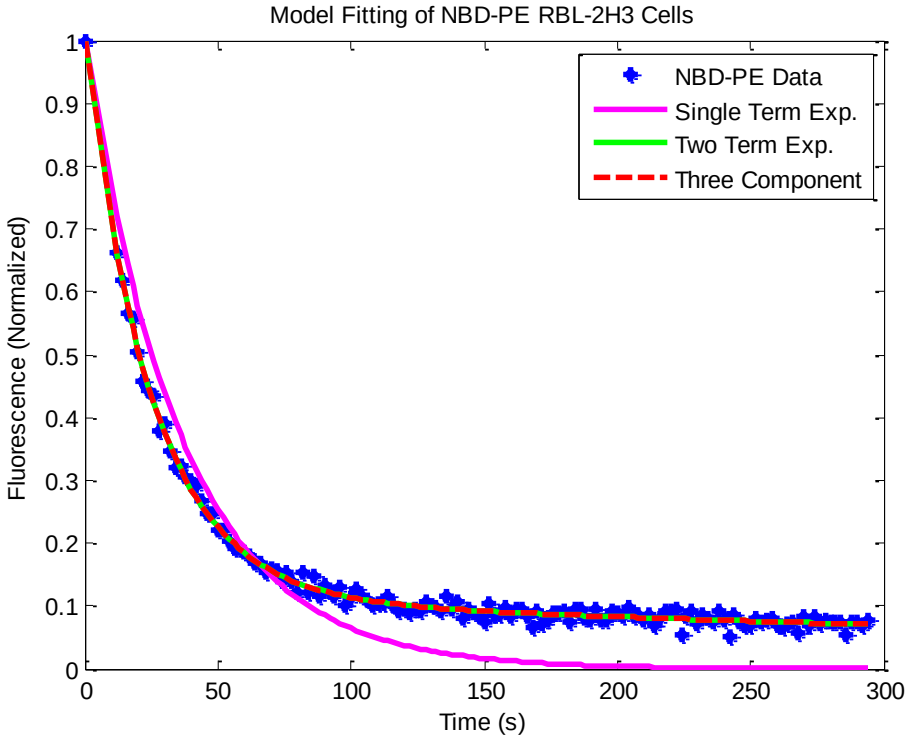

B

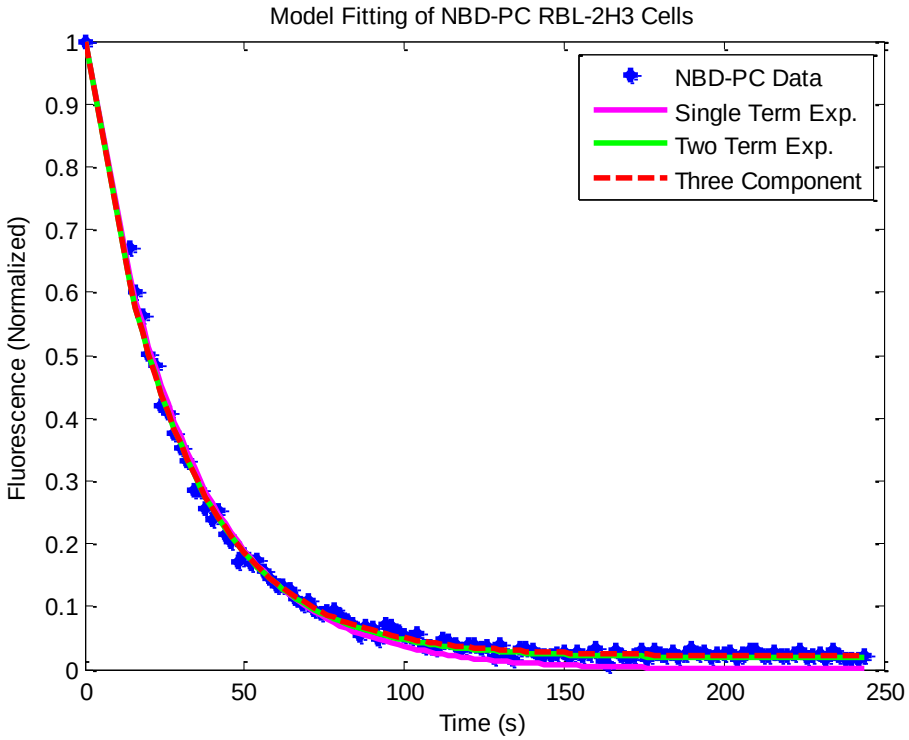

Figure 20 - Single term exponential, two term exponential, and three component model fits for (A) NBD-PE labeled and (B) NBD-PC labeled RBL-2H3 cells.

We find that the dithionite quenching behavior for NBD-PE labeled cells fits best to a two term exponential function and three component model while a single exponential is adequate for fitting the quenching behavior of NBD-PC labeled cells (Table 3). This may indicate that multiple components are necessary, one of which may be flippase activity, for describing the total quenching behavior of NBD-PE labeled cells. On the other hand, the quenching behavior of NBD-PC labeled cells may indicate that a single fast quenching component exists and may correspond solely to fluorescent NBD-PC reduction by dithionite.

For both NBD-PE and NBD-PC labeled cells, we find that the fast rate constant corresponding to fluorescent NBD reduction by dithionite has a half-time ($t_{1/2} = \ln(2)/k_i$) of approximately 20 seconds. The best fit rate constants for outward phospholipid flipping is found to have a half-time of approximately 6 minutes for NBD-PE labeled cells. The outward flipping constants for NBD-PC labeled cells are negligible, which may be due to the fact that the model fits imply that nearly all of the initial fluorescent NBD-PC are situated on the outer leaflet at the beginning of the assay. The inward flipping rates of both NBD-PE ($t_{1/2,in}$ = 315.1 s) and NBD-PC ($t_{1/2,in}$ = 866.4 s) labeled cells in our three component model seem to widely vary, although much like the GPMV dithionite assays, this model may not be able to provide an accurate indication of inward flipping due to rapid fluorescence reduction by dithionite. This rapid dithionite quenching component may obscure the rate of inward flipping as only quenched fluorophores are flipped to the inner leaflet.

Single Term Exponential $F(t) = e^{-kt}$

Label	k (s^{-1})	$t_{1/2}$ (s)	R^2
NBD-PE	0.02738	25.32	0.7687
NBD-PC	0.03324	20.85	0.9848

Two Term Exponential $F(t) = ae^{-k_{quench}t} + be^{-k_{out}t}$

Label	a	b = 1 - a	$(PL_{in})_i$	$(PL_{out})_i$	k_{quench} (s^{-1})	k_{out} (s^{-1})	$t_{1/2, kquench}$ (s)	$t_{1/2, kout}$ (s)	R^2
NBD-PE	0.8845	0.1155	0.1106	0.8894	0.04001	0.001683	17.32	411.9	0.9952
NBD-PC	0.9782	0.0218	0.0218	0.9782	0.03566	1.042×10^{-6}	19.44	6.652×10^{5}	0.9958

Three Component Model

Label	$(PL_{in})_{initial}$	$(PL_{out})_{initial}$	k_{quench} (s^{-1})	k_{in} (s^{-1})	k_{out} (s^{-1})	$t_{1/2, kquench}$ (s)	$t_{1/2, kin}$ (s)	$t_{1/2, kout}$ (s)	R^2
NBD-PE	0.0554	0.9446	0.0377	0.0022	0.0018	18.39	315.1	385.1	0.9952
NBD-PC	0.0000	1.0000	0.0350	0.0008	0.0007	19.80	866.4	990.2	0.9957

Table 3 – Single term exponential, two term exponential, and three-component model fit parameters for NBD-PE and NBD-PC labeled RBL-2H3 cells. Half-times ($t_{1/2}$) = ln(2)/k_i, where k_i represents the respective rate constants k, k_{in}, k_{out}, and k_{quench}.

We must interpret these results with the same considerations as with the dithionite quenching assays in the GPMVs. The possibility that dithionite is permeable to the cells would alter the proposed mechanistic model that is used to generate the quenching behavior rate constants. A possible method in which to assess dithionite permeability in cells would be to allow endocytosis of fluorescently labeled cell membranes and test whether dithionite treatment has altered quenching effects. Considerations that the NBD-PL labeled cells may not attain a steady state distribution of fluorescent phospholipids must also be taken into account which could be tested by performing dithionite assays with cells at various time points after incorporation of the fluorescent phospholipids. As with the GPMVs, these considerations must be addressed in order to make confident quantitative conclusions on the best fit rate constants and initial phospholipid

distributions. However, we may still be able to qualitatively conclude that the near complete quenching behavior observed in the NBD-PE labeled RBL-2H3 cells suggests multiple components in the quenching kinetics and one of these components may be attributed to flippase activity. The NBD-PC labeled cells also demonstrate near complete quenching although the single exponential fit suggest only a dithionite quenching component. Flippase mediated maintenance of NBD-PC at the outer leaflet is a possible explanation of this observation although this cannot be determined solely with these particular results.

3.2.2 Collisional Quenching Assays in RBL-2H3 Cells

Collisional quenching assays using Co^{2+} were conducted to examine whether and how the active flippase proteins were distributing the exogenously added NBD-PLs across the bilayer leaflets (Figure 21). For cells labeled with NBD-PE, there seems to be some apparent inaccessibility of the Co^{2+} quencher to a fraction of fluorophores as the quenching effects appear to level out at higher concentrations. This effect is not as apparent with the NBD-PC labeled cells however, Stern-Volmer analysis of these trends is necessary to quantify these observations.

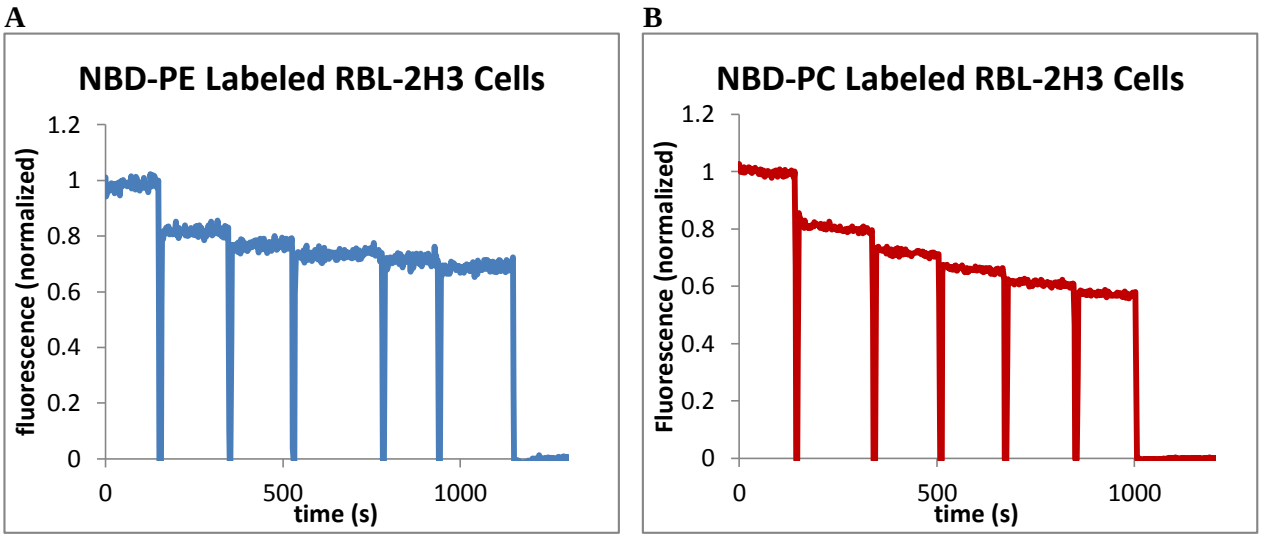

Figure 21 – Co^{2+} quenching titrations at 2 mM quencher concentration intervals of NBD-PL labeled RBL-2H3 cells. (A) Collisional quenching titration assay of NBD-PE labeled cells suggest that some fraction of fluorophores is inaccessible to the quencher and may be sequestered at the inner leaflet. (B) NBD-PC labeled cells seem to have a larger quencher-accessible fraction of fluorophores possibly being maintained at the outer leaflet.

Analyzing the titration data using Stern-Volmer relations, we can examine the distribution of NBD-PLs possibly due to the active flippases (Figure 22). In Stern-Volmer plots (Figure 22A), near-linearity of the NBD-PC labeled RBL-2H3 cells suggest that much of the PC is maintained on the outer leaflet of the bilayer. The non-linear behavior of the NBD-PE labeled cells suggest that some fraction of the PE is maintained at the inner leaflet of the bilayer. Using the modified Stern-Volmer equation, we calculate that approximately 57% of the NBD-PC is accessible to our collisional quencher whereas only approximately 35% of the NBD-PE is quencher accessible (Figure 22B).

A

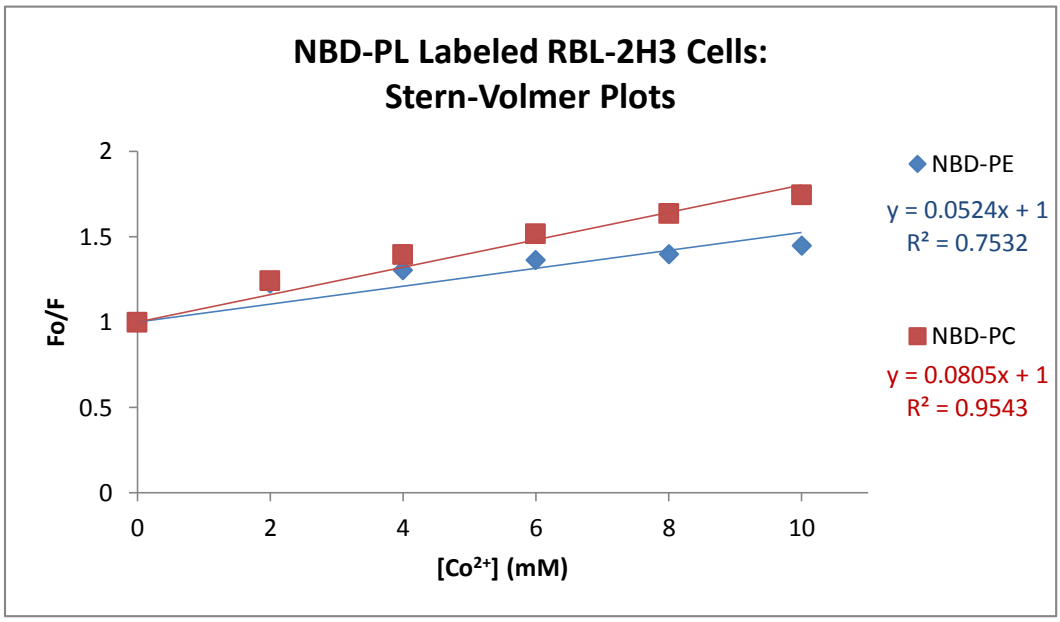

B

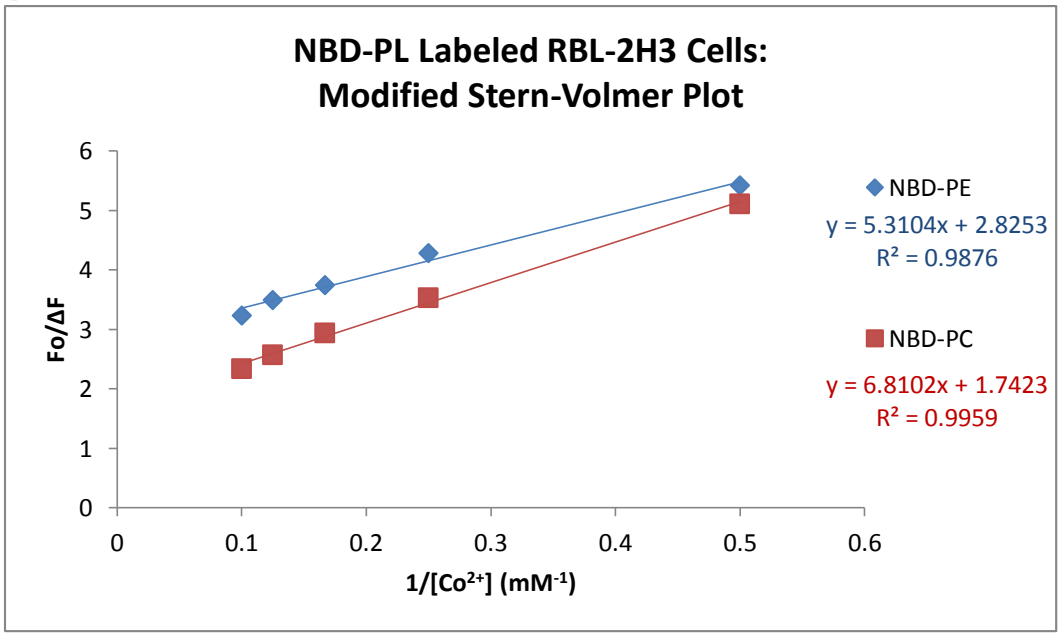

Figure 22 – (A) Stern Volmer plots show a rather linear quenching behavior of the NBD-PC labeled RBL-2H3 cells while the NBD-PE labeled cells exhibit a non-linear behavior indicating that some NBD-PE fluorophores are inaccessible to the quencher. (B) By modifying the Stern Volmer equation, we can plot fluorescence as an inverse function of quencher concentration. The y-axis intercept in this modified plot indicates the inverse fraction of fluorophores which are accessible to the collisional quencher and may correlate to fluorophores being maintained at the outer leaflet. We find that approximately 35% of the NBD-PE is quencher accessible while approximately 57% NBD-PC is quencher accessible.

Unlike the Co^{2+} quenching experiments with the GPMVs, the cations do not seem to have the same indications of permeability in these intact cell experiments. This is suggested by the observation that after addition of a particular concentration of collision quencher, the fluorescence signal is quickly reduced and seems to more rapidly stabilize before the next titration addition. The relative membrane impermeability of the Co^{2+} seen with these intact cells allows for greater confidence in correlating quencher accessibility with outer leaflet association of the fluorophores. As indicated above, we see that approximately 35% of the NBD-PE seems to be maintained at the outer bilayer leaflet while approximately 57% of the NBD-PC is maintained at the outer leaflet. The sequestering of NBD-PE at the inner leaflet seems to be consistent with the general distribution of amino-phospholipids at the plasma membrane [40]. In contrast, the majority of PC phospholipids is expected to be at the plasma membrane outer leaflet in intact cells. Our results with these NBD-PLs are qualitatively consistent with these expectations.

Much like the Co^{2+} collisional quenching experiments using the NBD-PE labeled GPMVs, we need to consider the possibility that insufficient time is allowed for an equilibrium distribution of the exogenously added NBD-PLs. If such was the case, more fluorophores would be available to the quencher at earlier time points in the experiment and the Stern-Volmer analysis may be predisposed towards non-linear behavior. However, the fact that we observe the fluorescence signal to stabilize after each addition of quencher in our titrations may argue against this concern. In addition, the heavily weighted low concentration values in our modified Stern-Volmer analysis due to the dependency of the inverse concentration of Co^{2+} may bias the calculated

fraction of quencher accessible fluorophores. Separate experiments designed to address these issues are necessary in order to enhance confidence in the interpretation of our results.

TX-100 and OG detergent permeabilization of the NBD-PL labeled RBL-2H3 cells was observed to have the same enhancement of fluorescence and quencher insensitivity as seen in the GPMVs, the latter of which made it problematic for analyzing the extent of flippase activity in this manner.

3.3 Antigen Stimulated and Reagent Mediated PS Flipping in RBL-2H3 Cells

While the quenching assays in GPMVs and in unstimulated RBL-2H3 cells give us indications on the function and kinetics of active flippases, we would like to explore methods in which to influence the activity of flippases in our RBL-2H3 cells. In this set of experiments, we tested means to induce or enhance flippase mediated exposure of PS by stimulating the intact cells using a variety of methods. These cell perturbation experiments may allow us to better understand the sensitivities of flippases and may provide further characterization opportunities when assessed together with our quenching experiments.

3.3.1 Antigen Stimulation of RBL-2H3 Cells

Antigen stimulation of RBL-2H3 mast cells causes aggregation of IgE-bound FcεRI receptors and initiates a signaling response that leads to degranulation events [41]. Activated RBL-2H3 cells also expose PS to the outer leaflet in proportion to the amount of degranulation [31]. Upon dinitrophenylated-bovine serum albumin (DNP-BSA) stimulation of anti-DNP IgE-sensitized

RBL-2H3 cells, PS exposure was observed using fluorescent Alexa Fluor 488 (AF488) Annexin V conjugate and was found to be punctate at the plasma membrane of the cells (Figure 23).

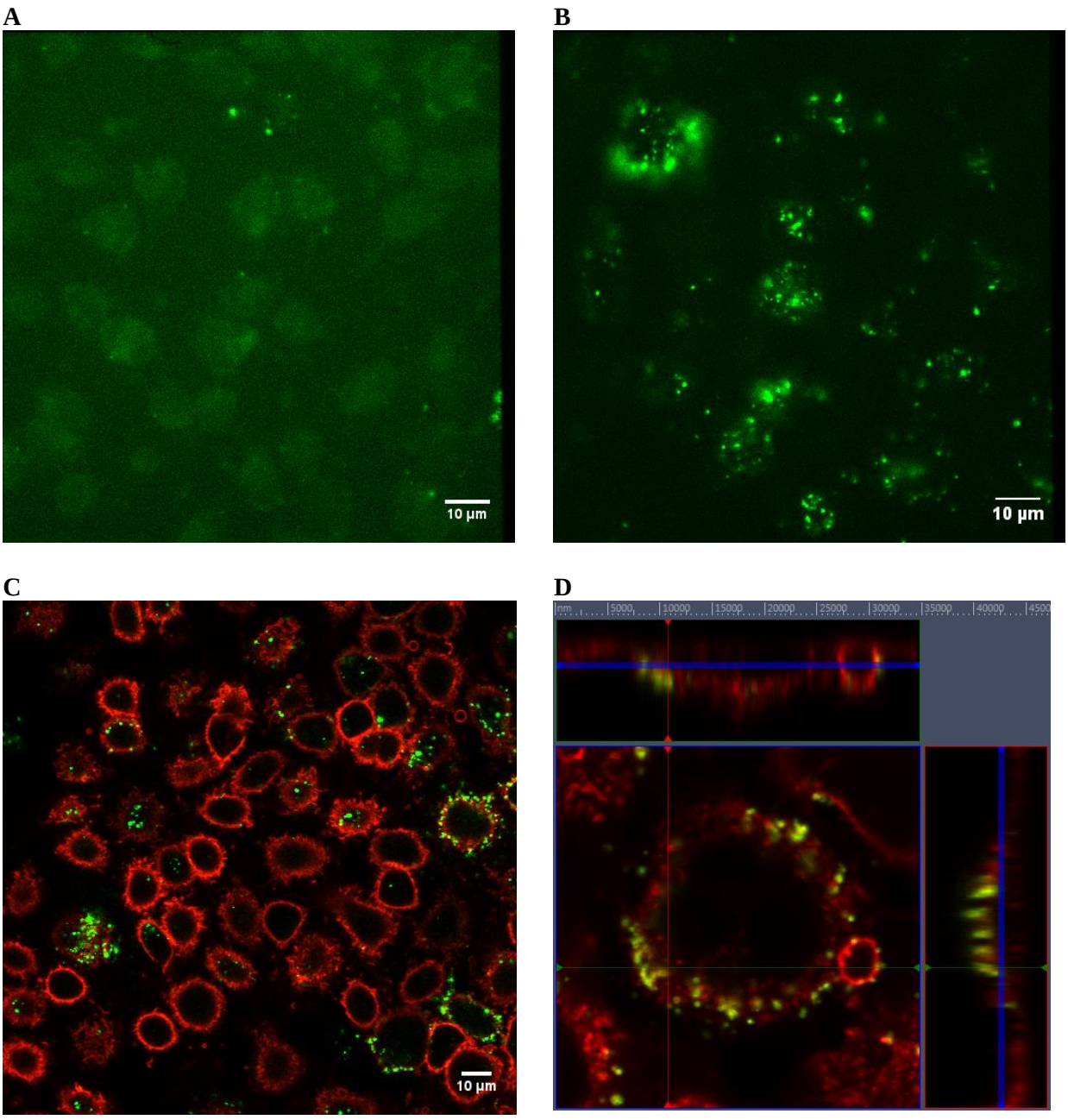

Figure 23 – (A) Unstimulated cells do not have PS exposed as no binding of Annexin V is observed. (B) Widefield fluorescence and (C and D) confocal microscopy images of antigen stimulated cells demonstrate punctated PS on the membrane surface as detected by Annexin V binding (green). Membrane staining using AF555 cholera toxin B (red), which binds to ganglioside GM1 [42, 43], was used to provide contrast.

3.3.2 Calcium Ionophore Treatment of RBL-2H3 Cells

Mast cell degranulation can also be induced by directly increasing intracellular calcium levels using calcium ionophore A23187 [44]. PS exposure of A23187-activated RBL-2H3 cells was found to be similarly punctate at the plasma membrane, but perhaps less robust than PS exposure in antigen stimulated cells (Figure 24). The punctate nature of PS exposure in antigen stimulated and calcium ionophore treated cells is not well understood, although there have been attempts in observing co-localization of PS to lipid raft regions [43] as well as sites of exocytosis [31] with varying degrees of confidence.

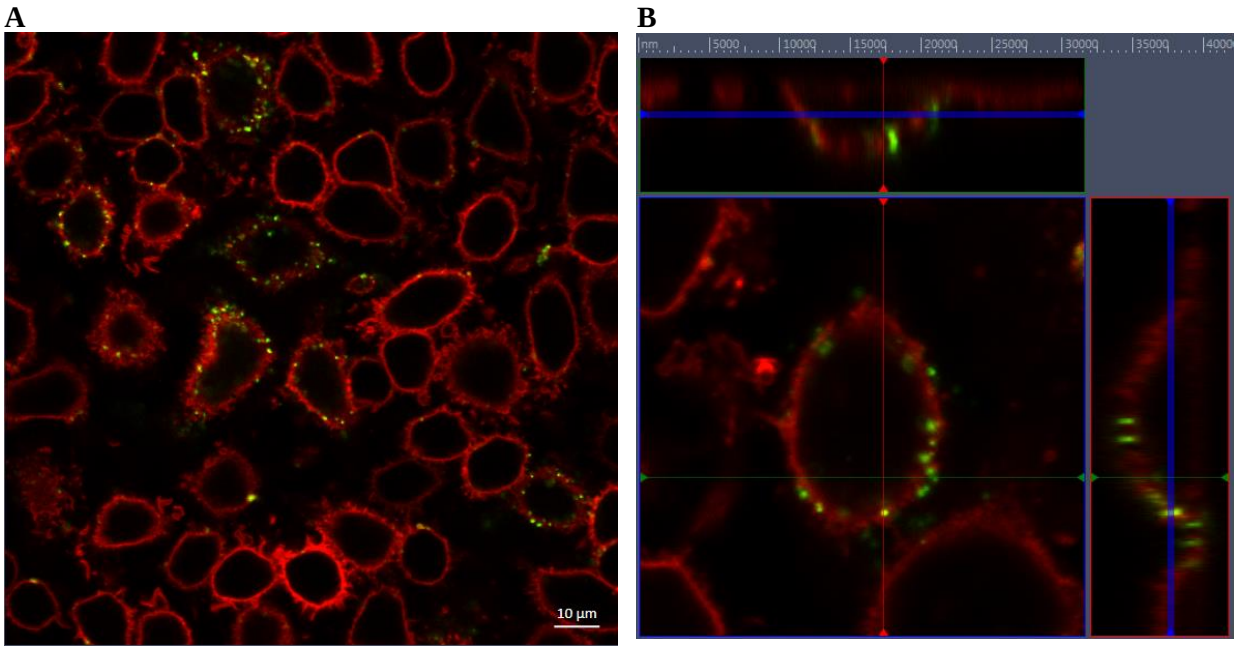

Figure 24 – (A and B) Confocal images of A23187 treated cells demonstrate punctated PS exposure on the membrane as detected by AF488 Annexin V binding (green). Membrane staining using AF555 cholera toxin B (red) was used to provide contrast.

3.3.3 Cholesterol Depletion of RBL-2H3 Cells

Membrane cholesterol levels have been suggested to have an impact on PS exposure in erythrocyte cells [45]. Zwieten et. al demonstrated that cholesterol depletion of erythrocytes enhanced PS exposure, while cholesterol loading of cells decreased PS exposure. In order to examine the effects of cholesterol depletion in RBL-2H3 cells, cells where treated with methyl-β-cyclodextrin and PS exposure was monitored (Figure 25). Increased PS exposure was detectable although not to the same extent as antigen stimulated and calcium ionophore treated cells. The relation between membrane cholesterol content and PS exposure is not well understood. It is possible that reducing cholesterol levels at the plasma membrane enhances membrane fluidity [45], which may have some direct effects on the energy-barrier for phospholipid flipping [46] or even the flippase mechanism itself [47]. Speculation can also be made regarding the relation between PS and cholesterol-rich lipid raft domains, as cholesterol depletion has been demonstrated to largely affect these ordered membrane regions in living cell membranes [48].

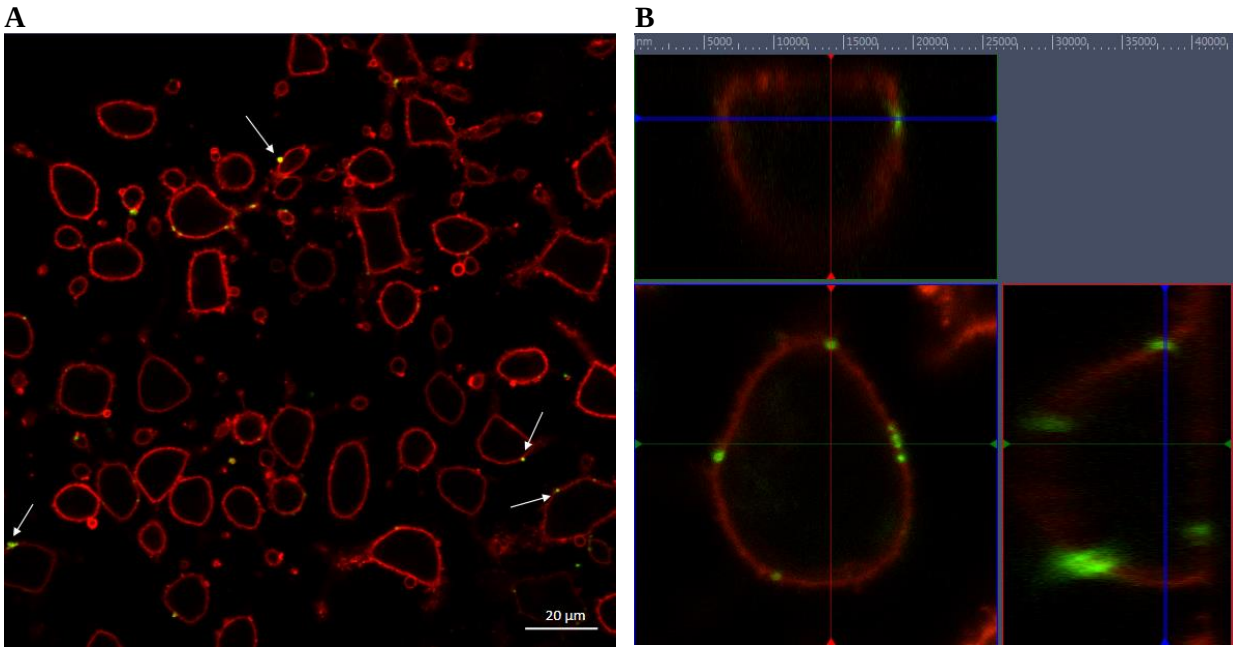

Figure 25 – (A and B) Cholesterol was depleted from RBL-2H3 cells using methyl-β-cyclodextrin. PS exposure in these confocal images was observed to be scattered about the membrane as indicated by AF488 Annexin V binding. (A) Arrows indicate select regions of PS exposure.

3.3.4 NEM Treatment of RBL-2H3 Cells

The cysteine modification reagent N-ethylmaleimide (NEM) has been shown to inhibit some flippase activity in reconstituted-proteoliposomes [49]. NEM treated RBL-2H3 cells displayed pronounced PS exposure (Figure 26) possibly by the chemical inactivation of uni-directional flippases that maintain bilayer asymmetry. This observed PS exposure was found to be rather continuous about the plasma membrane rather than punctate in behavior such as in the activated RBL-2H3 cells. Conversely, Chang et al. [49] demonstrated that NEM inhibition of ER flippases only occurred when the flippase proteins were treated while solubilized in TX-100 extract as tested in their proteoliposomes systems. It was argued that the NEM sensitive critical cysteine(s) in ER flippase proteins are buried in the membrane and inaccessible to the modifying reagent. We find that the particular flippase residue or characteristic that is sensitive to NEM is accessible in our RBL-2H3 cells. This may indicate that there are distinctly different flippases regulating PS

in the ER than at the plasma membrane. However, caution should be taken when considering this suggestion as the proteoliposomes system has considerable dissimilarity from our RBL-2H3 cells.

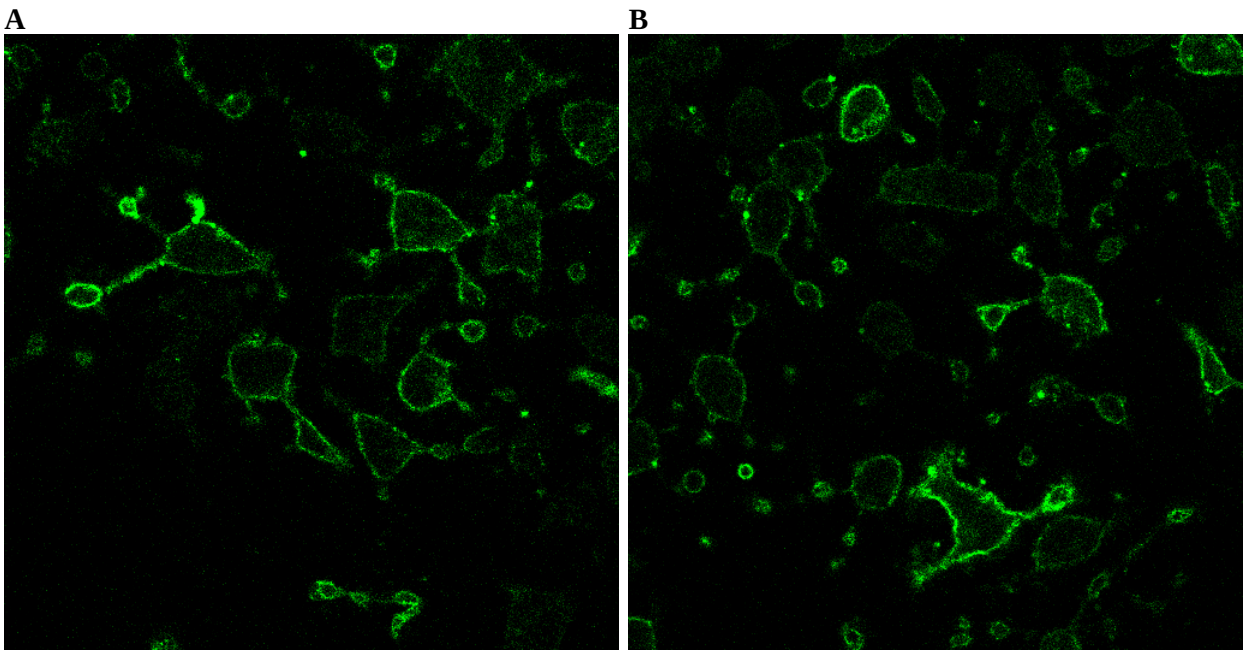

Figure 26 – (A and B) Confocal images of NEM treated RBL-2H3 cells exhibit distinct and continuous PS labeling on the surface of the membrane as detected by AF488 annexin V binding.

CHAPTER 4 – CONCLUSIONS AND FUTURE DIRECTIONS

4.1 Flippase Activity in GPMVs

Our quenching experiments with NBD-PL labeled GPMVs suggest flippase activity. Model fitting of the quenching behavior indicates that multiple components are necessary for describing the near complete quenching. One of these components may to be attributed to fast dithionite reduction of the fluorescent NBD derivatives ($t_{1/2,\ quench} = \ln(2)/k_{quench} < 1$ minute), while other components of the quenching behavior seems to indicate slower, potentially flippase mediated translocation of fluorescent phospholipids. In our model fits, we find that the outward flipping mechanism has a half-time of approximately 8 - 11 minutes. The inward flipping rate is found to be relatively insignificant compared to the rapid dithionite reduction of outer leaflet fluorophores. This may be because only non-fluorescent phospholipids are flipped inwards and therefore our assay may not be able to provide a relevant measurement for inward phospholipid flipping kinetics. These results suggest flippase activity, but we may only be able to interpret them as a qualitative indicator due to untested concerns of potential dithionite membrane permeability and non-steady state distribution of fluorescence NBD-PLs.

Collisional quenching experiments using Co^{2+} divalent cations can be used as a measure of phospholipid distribution across membrane bilayer leaflets. After exogenous NBD-PE incorporation into our GPMVs, titrations of Co^{2+}, which should quench fluorescent phospholipids only on the extracellular leaflet, seemed to indicate that a portion of the NBD-PE fluorophores were sequestered to the inner membrane leaflet. This is inferred by the bi-phasic Co^{2+} quenching behavior observed in our titrations, our individually quenched samples, and by

analysis via Stern-Volmer relations. Modified Stern-Volmer plots indicate that a fraction of the NBD-PE is inaccessible to the quencher. However, the Co^{2+} quenching at higher concentrations show a slow, linear behavior which may suggest membrane permeability of the divalent cations and complicate our analysis. This type of permeability at higher Co^{2+} concentrations has also been observed in collisional quenching experiments using PS-PE vesicles [38] however, separate experiments using PC-PE-PS-SM lipid vesicles found that Co^{2+} was membrane impermeable [33]. Although we are not able to conclusively determine the distribution of NBD-PE in our GPMVs, the indication that NBD-PE is distributed into both bilayer leaflets to some extent suggests that active membrane flippases mediate this movement.

Efforts to directly permeabilize NBD-PE labeled GPMVs were met with additional difficulties. By permeabilizing the fluorescently labeled GPMVs, we would expect enhanced quenching with titrations of Co^{2+} as fluorophores on both leaflets of the bilayer should be near equally accessible. However, membrane permeabilization using saponin exhibited a minimal enhancement of quenching while TX-100 and octyl glucoside permeabilization demonstrated a rapid enhancement of fluorescence signal after addition of the detergents. Octyl glucoside solubilization of the GPMVs also was found to produce a relative insensitivity to the Co^{2+} quencher. These detergent solubilization effects make it difficult to use detergent permeabilization methods effectively in determining flippase mediated phospholipid distribution in GPMVs.

4.2 Flippase Activity in RBL-2H3 Cells

The results from the GPMV experiments were substantial enough to proceed in testing for flippase activity in intact RBL-2H3 cells. Dithionite quenching assays exhibited near complete quenching for RBL-2H3 cells labeled with both NBD-PE and NBD-PC. The quenching behavior of cells labeled with NBD-PC was adequately fit to a single term exponential, which may be attributed solely to dithionite reduction of the fluorescent phospholipids. This seems to indicate that nearly all of the NBD-PC is located at the outer leaflet although it unclear if this is flippase mediated or not. Cells labeled with NBD-PE were found to have quenching behavior that fit a multi-component model, indicating that a possible flippase mediated component contributes to the near complete quenching. From our models, we find that the outward flipping mechanism has a half-time of approximately 6.5 minutes. The inward flipping rate is found to be relatively insignificant compared to the rapid dithionite reduction of outer leaflet fluorophores which allow only non-fluorescent phospholipids to be flipped inwards and therefore may obscure an accurate value of inwards phospholipid flipping. In both the NBD-PE and NBD-PC labeled cells, the fast dithionite reduction of the fluorescent NBD derivatives is found to have a half-time of approximately 20 seconds. As with the results from the GPMV dithionite quenching assays, we may only be able to interpret these results as a qualitative indicator of flippase activity due to untested concerns of potential dithionite membrane permeability and non-steady state distribution of fluorescence NBD-PLs.

Co^{2+} collisional quenching experiments with the RBL-2H3 cells suggested a distinct distribution of membrane phospholipids using the exogenously incorporated NBD-PLs. In NBD-PE labeled cells, a significant fraction of inaccessible fluorophores was suggested to be maintained at the

inner leaflet. Examination of the collisional quenching using Stern-Volmer relations found that approximately 65% of the NBD-PE fluorescent phospholipids were sequestered to the inner leaflet while approximately 43% of the NBD-PC fluorophores were found at the inner leaflet. This distribution of PE phospholipid analogues is qualitatively consistent with the typical asymmetry of plasma membranes [3], although we may expect that a larger majority of PC phospholipid analogues to be maintained at the outer leaflet. Considerations of Co^{2+} membrane permeability were minimized as with of each aliquot of quencher, the fluorescence decrease was sudden and was effectively stabilized before the next addition of Co^{2+}. However, steady state considerations remain untested and may limit us in concluding that these results only suggest flippases are distributing the NBD-PLs in some manner across the bilayer.

4.3 Monitoring PS Translocation in Antigen Stimulated and Chemically Perturbed RBL-2H3 Cells

Using Annexin V binding assays, PS flipping was effectively monitored in cells under selected conditions related to cell activation and membrane environment. In untreated cells, antigen stimulation caused robust, punctate PS on the cell surface, which has also been observed in previous studies [31, 50]. PS was found to be sequestered to the inner leaflet in non-stimulated RBL-2H3 cells, as indicated by the absence of annexin V binding. Increasing cytosolic calcium levels using A23187 calcium ionophore was also found to enhance PS exposure in a punctated manner at the extracellular cell surface. A23187 treatment of mast cells has been found to exhibit a similar degranulation response as antigen stimulated cells [44].

Depletion of plasma membrane cholesterol using methyl-β-cyclodextrin was found to slightly enhance PS exposure of inactive cells. These results are consistent with the observation that cholesterol depletion in erythrocyte cells also enhances PS cell surface exposure in the presence of extracellular calcium [45]. This effect may be related to cholesterol's functionality in ordering of membrane lipids, as cholesterol depletion may enhance fluidity of the phospholipid bilayer and effectively lower the energy barrier for phospholipid translocation. As cholesterol is abundant in plasma membrane ordered-domains [48], there may also be a relation between flippases that mediate PS exposure and lipid raft regions characterized in this manner.

NEM treated cells displayed prominent PS plasma membrane exposure in inactive cells that was comparably more continuous than punctate in behavior as compared to PS exposure in activated cells. This cysteine modification reagent was reported previously to inactivate some fraction of ER flippases but only when the proteins are TX-100 extracted and treated with NEM before reconstitution in liposomes [49]. Our results indicate that NEM may be able to inactivate uni-directional flippase(s) whose substrate is PS in cell membranes, which may suggest that flippases that mediate PS exposure at the ER are distinct from those at the plasma membrane.

4.4 Future Directions

The experiments described in this document indicate that flippase activity can be readily studied in GPMV and RBL-2H3 cells. In order to improve upon these results and explore new properties of flippase proteins, both quenching and Annexin V binding assays can be employed in new variations.

Co^{2+} membrane permeation may be measured using fluorescently labeled NBD-glucose. This glucose analog can be incorporated intracellulary into GPMVs or cells and the cytoplasmic accessibility of Co^{2+} can be inferred by the extent of fluorescence quenching. This type of data would be supportive in confirming the results of our collisional quenching assays that seem to demonstrate flippase mediated activity in our RBL-2H3 cell membranes and GPMVs.

Utilizing other NBD-PL analogs in our fluorescence quenching assays, such as NBD-Phosphatidylserine (NBD-PS) and NBD-Sphingomyelin (NBD-SM), may demonstrate bilayer asymmetry of different phospholipids in our GPMVs and RBL-2H3 cells. Kinetic measurements using dithionite quenching assays of other NBD-PL labeled membranes may find new characteristics of flippases that vary in the speed of their functionality based on their particular substrates. These quenching assays may also be used in conjunction with cell stimulation methods to further characterize the behavior of flippases in the plasma membrane.

The effects of diethylpyrocarbonate (DEPC), a histidine modification reagent, may be studied in the context of phosphatidylserine exposure in RBL-2H3 cells. DEPC has been shown to inhibit a subset of ER flippase proteins [49] and may have similar effects with plasma membrane flippases in RBL-2H3 cells. Additional characterization of plasma membrane flippases in our RBL-2H3 cells may contribute in the effort to identifying new proteins with flippase activity and may illuminate their functional mechanism.

APPENDIX A: Two Exponential Analytical Derivation

$$PL_{in} \xrightarrow{k_{out}} PL_{out} \xrightarrow{k_{quench}} PL_{quenched}$$

$\frac{dPL_{in}}{dt} = -k_{out}(PL_{in})$ (Equation 1)

$\frac{dPL_{out}}{dt} = k_{out}(PL_{in}) - k_{quench}(PL_{out})$ (Equation 2)

$\frac{dPL_{quenched}}{dt} = k_{quench}(PL_{out})$ (Equation 3)

Initial Conditions:

$(PL_{in})\,(t = 0) = (PL_{in})_i$ (Initial Condition 1)

$(PL_{out})\,(t = 0) = (PL_{out})_i$ (Initial Condition 2)

$(PL_{quenched})\,(t = 0) = 0$ (Initial Condition 3)

From Equation 1, we can solve the differential equation by applying Initial Condition 1 to find that:

$PL_{in} = (PL_{in})_i e^{-k_{out}t}$ (Equation 4)

We can substitute Equation 4 into Equation 2 to find:

$\frac{dPL_{out}}{dt} + k_{quench}(PL_{out}) = k_{out}(PL_{in})_i e^{-k_{out}t}$ (Equation 5)

Equation 5 has the form $y'(t) + p(t)y(t) = q(t)$, where $p(t) = k_{quench}$ and

$q(t) = k_{out}(PL_{in})_i e^{-k_{out}t}$. We can use the general solution $y(t) = \frac{\int u(t)q(t)dt + Constant}{u(t)}$ where $u(t) = \exp[\int p(t)dt]$.

We now find that:

$$u(t) = \mathrm{e}^{k_{quench}t} \qquad \text{(Equation 6)}$$

$$PL_{out}(t) = \frac{\int \mathrm{e}^{k_{quench}t} k_{out}(PL_{in})_i e^{-k_{out}t} dt + Constant}{\mathrm{e}^{k_{quench}t}}$$

$$= \frac{k_{out}(PL_{in})_i e^{\left(k_{quench}-k_{out}\right)t}}{(k_{quench}-k_{out})\mathrm{e}^{k_{quench}t}} + \frac{Constant}{\mathrm{e}^{k_{quench}t}} \qquad \text{(Equation 7)}$$

Applying Initial Condition 2 to Equation 7, we find that:

$$Constant = (PL_{out})_i - \frac{k_{out}(PL_{in})_i}{(k_{quench}-k_{out})}$$

Substituting the Constant into Equation 7, we have:

$$PL_{out}(t) = \left((PL_{out})_i - \frac{k_{out}(PL_{in})_i}{(k_{quench}-k_{out})}\right)\mathrm{e}^{-k_{quench}t} + \left(\frac{k_{out}(PL_{in})_i}{(k_{quench}-k_{out})}\right)e^{-k_{out}t} \qquad \text{(Equation 8)}$$

Finally, our total fluorescence F(t) is the sum of Equations 4 and 8

$$F(t) = (PL_{in})_i e^{-k_{out}t} + \left((PL_{out})_i - \frac{k_{out}(PL_{in})_i}{(k_{quench}-k_{out})}\right)\mathrm{e}^{-k_{quench}t} + \left(\frac{k_{out}(PL_{in})_i}{(k_{quench}-k_{out})}\right)e^{-k_{out}t}$$

Which can be simplified to:

$$F(t) = aexp^{-k_{quench}t} + bexp^{-k_{out}t} \qquad \text{(Equation 9)}$$

Where $a = (PL_{out})_i - \frac{k_{out}(PL_{in})_i}{(k_{quench}-k_{out})}$ and $b = (PL_{in})_i + \left(\frac{k_{out}(PL_{in})_i}{(k_{quench}-k_{out})}\right)$

APPENDIX B: Modified Stern-Volmer Equation

Definitions:

F_o = fluorescence in the absence of quencher

$F_{o,a}$ = fluorescence of an accessible fluorophore population (in absence of quencher)

$F_{o,b}$ = fluorescence of an inaccessible fluorophore population (in absence of quencher)

[Q] = quencher concentration

K = Stern Volmer Constant

Derivation:

$$F = \frac{F_{o,a}}{1+k[Q]} + F_{o,b} \qquad (1)$$

Equation 1 is just showing that the fluorescence is a function of the quencher concentration but the quencher concentration has no effect on the fluorescence of the inaccessible fluorophore (Fob). The total initial fluorescence is the sum of the initial fluorescence of both populations of fluorophores.

$$F_o = F_{o,a} + F_{o,b} \qquad (2)$$

Now we define: $\Delta F = F_o - F$ and plug in equations 1 and 2 to get

$$\Delta F = F_{o,a} + F_{o,b} - \left(\frac{F_{o,a}}{1+k[Q]} + F_{o,b}\right) = F_{o,a} - \frac{F_{o,a}}{1+k[Q]} = F_{o,a}\left(1 - \frac{1}{1+K[Q]}\right) = F_{o,a}\left(\frac{K[Q]}{1+K[Q]}\right)$$

So now $$\Delta F = F_{o,a}\left(\frac{K[Q]}{1+K[Q]}\right) \qquad (3)$$

We can take equation 2 and divide it by equation 3

$\frac{F_o}{\Delta F} = \frac{F_{o,a}+F_{o,b}}{F_{o,a}\left(\frac{K[Q]}{1+K[Q]}\right)}$ we know the fraction of accessible fluorophores $f_a = \frac{F_{o,a}}{F_{o,a}+F_{o,b}}$ so now we have

$$\frac{F_o}{\Delta F} = \frac{1}{f_a}\left(\frac{1+K[Q]}{K[Q]}\right) = \frac{1}{f_a}\left(\frac{1}{K[Q]} + \frac{K[Q]}{K[Q]}\right) = \frac{1}{f_a}\left(\frac{1}{K[Q]} + 1\right)$$

So our modified Stern Volmer Equation is: $$\frac{F_o}{\Delta F} = \frac{1}{f_a}\frac{1}{K[Q]} + \frac{1}{f_a} \qquad (4)$$

REFERENCES

1. Singer, S. Jonathan, and Garth L. Nicolson. "The fluid mosaic model of the structure of cell membranes." *Science* 175.23 (1972): 720-731.
2. Alberts B, Johnson A, Lewis J, et al. Molecular Biology of the Cell. 4th edition. New York: Garland Science; 2002. The Lipid Bilayer. Available from: http://www.ncbi.nlm.nih.gov/books/NBK26871/
3. Zachowski, Alain. "Phospholipids in animal eukaryotic membranes: transverse asymmetry and movement." *BIOCHEMICAL JOURNAL-LONDON*- 294 (1993): 1-1.
4. Fadok, VALERIE A., et al. "Exposure of phosphatidylserine on the surface of apoptotic lymphocytes triggers specific recognition and removal by macrophages." *The Journal of Immunology* 148.7 (1992): 2207-2216.
5. Bevers, Edouard M., Paul Comfurius, and Robert FA Zwaal. "Changes in membrane phospholipid distribution during platelet activation." *Biochimica et Biophysica Acta (BBA) - Biomembranes* 736.1 (1983): 57-66.
6. Di Paolo, Gilbert, and Pietro De Camilli. "Phosphoinositides in cell regulation and membrane dynamics." *Nature* 443.7112 (2006): 651-657.
7. McConnell, Harden M., and Roger D. Kornberg. "Inside-outside transitions of phospholipids in vesicle membranes." *Biochemistry* 10.7 (1971): 1111-1120.
8. Pomorski, T., and A. K. Menon. "Lipid flippases and their biological functions." *Cellular and Molecular Life Sciences CMLS* 63.24 (2006): 2908-2921.
9. Palmgren, Michael G., and Poul Nissen. "P-type ATPases." *Annual review of biophysics* 40 (2011): 243-266.

10. Sebastian, Tessy T., et al. "Phospholipid flippases: building asymmetric membranes and transport vesicles." *Biochimica et Biophysica Acta (BBA) - Molecular and Cell Biology of Lipids* 1821.8 (2012): 1068-1077.
11. Zhou, Xiaoming, and Todd R. Graham. "Reconstitution of phospholipid translocase activity with purified Drs2p, a type-IV P-type ATPase from budding yeast." *Proceedings of the National Academy of Sciences* 106.39 (2009): 16586-16591.
12. Pomorski, Thomas, et al. "Drs2p-related P-type ATPases Dnf1p and Dnf2p are required for phospholipid translocation across the yeast plasma membrane and serve a role in endocytosis." *Molecular biology of the cell* 14.3 (2003): 1240-1254.
13. Coleman, Jonathan A., Michael CM Kwok, and Robert S. Molday. "Localization, purification, and functional reconstitution of the P4-ATPase Atp8a2, a phosphatidylserine flippase in photoreceptor disc membranes." *Journal of Biological Chemistry* 284.47 (2009): 32670-32679.
14. Higgins, Christopher F. "ABC transporters: from microorganisms to man." *Annual review of cell biology* 8.1 (1992): 67-113.
15. Coleman, Jonathan A., Faraz Quazi, and Robert S. Molday. "Mammalian P4-ATPases and ABC transporters and their role in phospholipid transport." *Biochimica et Biophysica Acta (BBA) - Molecular and Cell Biology of Lipids* 1831.3 (2013): 555-574.
16. van Helvoort, Ardy, et al. "MDR1 P-glycoprotein is a lipid translocase of broad specificity, while MDR3 P-glycoprotein specifically translocates phosphatidylcholine." *Cell* 87.3 (1996): 507-517.

17. Quazi, Faraz, and Robert S. Molday. "Differential Phospholipid Substrates and Directional Transport by ATP-binding Cassette Proteins ABCA1, ABCA7, and ABCA4 and Disease-causing Mutants." *Journal of Biological Chemistry* 288.48 (2013): 34414-34426.
18. Dekkers, D., et al. "Comparison between Ca2+-induced scrambling of various fluorescently labelled lipid analogues in red blood cells." *Biochem. J* 362 (2002): 741-747
19. Zhou, Quansheng, et al. "Molecular cloning of human plasma membrane phospholipid scramblase a protein mediating transbilayer movement of plasma membrane
20. Shettihalli, Ashok Kumar, and Sathyanarayana N. Gummadi. "Biochemical evidence for lead and mercury induced transbilayer movement of phospholipids mediated by human phospholipid scramblase 1." *Chemical research in toxicology* 26.6 (2013): 918-925.
21. Zhou, Quansheng, et al. "Normal hemostasis but defective hematopoietic response to growth factors in mice deficient in phospholipid scramblase 1."*Blood* 99.11 (2002): 4030-4038.
22. Bevers, Edouard M., and Patrick L. Williamson. "Phospholipid scramblase: an update." *FEBS letters* 584.13 (2010): 2724-2730.
23. Suzuki, Jun, et al. "Calcium-dependent phospholipid scramblase activity of TMEM16 protein family members." *Journal of Biological Chemistry* 288.19 (2013): 13305-13316.
24. Malvezzi, Mattia, et al. "Ca2+-dependent phospholipid scrambling by a reconstituted TMEM16 ion channel." *Nature communications* 4 (2013).
25. Kunzelmann, Karl, et al. "Molecular functions of anoctamin 6 (TMEM16F): a chloride channel, cation channel, or phospholipid scramblase?" *Pflügers Archiv-European Journal of Physiology* (2013): 1-8.
26. Menon, Indu, et al. "Opsin is a phospholipid flippase." *Current Biology* 21.2 (2011): 149-153.

27. Scott, R. E., et al. "Plasma membrane vesiculation in 3T3 and SV3T3 cells. I. Morphological and biochemical characterization." *Journal of cell science* 35.1 (1979): 229-243.
28. Holowka, David, and Barbara Baird. "Structural studies on the membrane-bound immunoglobulin E-receptor complex. 1. Characterization of large plasma membrane vesicles from rat basophilic leukemia cells and insertion of amphipathic fluorescent probes." *Biochemistry* 22.14 (1983): 3466-3474.
29. Passante, Egle, and Neil Frankish. "The RBL-2H3 cell line: its provenance and suitability as a model for the mast cell." *Inflammation research* 58.11 (2009): 737-745.
30. Holowka, David, and Barbara Baird. "Antigen-mediated IgE receptor aggregation and signaling: a window on cell surface structure and dynamics." *Annual review of biophysics and biomolecular structure* 25.1 (1996): 79-112.
31. Demo, S. D., et al. "Quantitative measurement of mast cell degranulation using a novel flow cytometric annexin-V binding assay." *Cytometry* 36.4 (1999): 340-348.
32. McIntyre, Jonathan C., and Richard G. Sleight. "Fluorescence assay for phospholipid membrane asymmetry." *Biochemistry* 30.51 (1991): 11819-11827.
33. Scaglione, Beth A., and D. A. Rintoul. "A fluorescence-quenching assay for measuring permeability of reconstituted lens MIP26." *Investigative ophthalmology & visual science* 30.5 (1989): 961-966.
34. Hrafnsdóttir, Sigrún, J. Wylie Nichols, and Anant K. Menon. "Transbilayer movement of fluorescent phospholipids in Bacillus megaterium membrane vesicles." *Biochemistry* 36.16 (1997): 4969-4978.

35. Vermes, István, et al. "A novel assay for apoptosis flow cytometric detection of phosphatidylserine expression on early apoptotic cells using fluorescein labelled annexin V." *Journal of immunological methods* 184.1 (1995): 39-51.
36. Sezgin, Erdinc, et al. "Elucidating membrane structure and protein behavior using giant plasma membrane vesicles." *Nature protocols* 7.6 (2012): 1042-1051.
37. Baumgart, Tobias, et al. "Large-scale fluid/fluid phase separation of proteins and lipids in giant plasma membrane vesicles." *Proceedings of the National Academy of Sciences* 104.9 (2007): 3165-3170.
38. Morris, Stephen J., Diane Bradley, and Robert Blumenthal. "The use of cobalt ions as a collisional quencher to probe surface charge and stability of fluorescently labeled bilayer vesicles." *Biochimica et Biophysica Acta (BBA)-Biomembranes* 818.3 (1985): 365-372.
39. Jamur, Maria Célia, and Constance Oliver. "Permeabilization of cell membranes." *Immunocytochemical Methods and Protocols*. Humana Press, 2010. 63-66.
40. Fadeel, Bengt, and Ding Xue. "The ins and outs of phospholipid asymmetry in the plasma membrane: roles in health and disease." *Critical reviews in biochemistry and molecular biology* 44.5 (2009): 264-277.
41. Blank, Ulrich, and Juan Rivera. "The ins and outs of IgE-dependent mast-cell exocytosis." *Trends in immunology* 25.5 (2004): 266-273.
42. Holmgren, Jan, et al. "Interaction of cholera toxin and membrane GM1 ganglioside of small intestine." *Proceedings of the National Academy of Sciences* 72.7 (1975): 2520-2524.
43. Fischer, Karin, et al. "Antigen recognition induces phosphatidylserine exposure on the cell surface of human CD8+ T cells." *Blood* 108.13 (2006): 4094-4101.

44. Hempstead, Barbara L., Anthony Kulczycki Jr, and Charles W. Parker. "Phosphorylation of the IgE receptor from ionophore A23187 stimulated intact rat mast cells." *Biochemical and biophysical research communications* 98.3 (1981): 815-822.

45. van Zwieten, Rob, et al. "The cholesterol content of the erythrocyte membrane is an important determinant of phosphatidylserine exposure." *Biochimica et Biophysica Acta (BBA)-Molecular and Cell Biology of Lipids* 1821.12 (2012): 1493-1500.

46. Anglin, Timothy C., et al. "Free energy and entropy of activation for phospholipid flip-flop in planar supported lipid bilayers." *The Journal of Physical Chemistry B*114.5 (2010): 1903-1914.

47. Langer, Marcella, et al. "Structural properties of model phosphatidylcholine flippases." *Chemistry & biology* 20.1 (2013): 63-72.

48. Hao, Mingming, Sushmita Mukherjee, and Frederick R. Maxfield. "Cholesterol depletion induces large scale domain segregation in living cell membranes." *Proceedings of the National Academy of Sciences* 98.23 (2001): 13072-13077.

49. Chang, Qing-long, Sathyanarayana N. Gummadi, and Anant K. Menon. "Chemical modification identifies two populations of glycerophospholipid flippase in rat liver ER." *Biochemistry* 43.33 (2004): 10710-10718.

50. Wu, Min, et al. "Differential targeting of secretory lysosomes and recycling endosomes in mast cells revealed by patterned antigen arrays." *Journal of cell science* 120.17 (2007): 3147-3154.